Eur. Phys. J. C 47, 815–831 (2006)
Digital Object Identifier (DOI) 10.1140/epjc/s2006-02602-y

THE EUROPEAN PHYSICAL JOURNAL C

The rare decays $B \to K^{(*)}\bar{K}^{(*)}$ and R-parity violating supersymmetry

R.M. Wang[1,2,a], G.R. Lu[1,2], E.-K. Wang[1], Y.-D. Yang[2,b]

[1] Institute of Particle Physics, Huazhong Normal University, Wuhan, Hubei 430070, P.R. China
[2] Department of Physics, Henan Normal University, XinXiang, Henan 453007, P.R. China

Received: 12 March 2006 /
Published online: 7 July 2006 –

Abstract. We study the branching ratios, the direct CP asymmetries in $B \to K^{(*)}\bar{K}^{(*)}$ decays and the polarization fractions of $B \to K^*\bar{K}^*$ decays by employing the QCD factorization in the minimal supersymmetric standard model with R-parity violation. We derive the new upper bounds on the relevant R-parity violating couplings from the latest experimental data of $B \to K^{(*)}\bar{K}^{(*)}$, and some of these constraints are stronger than the existing bounds. Using the constrained parameter spaces, we predict the R-parity violating effects on the other quantities in $B \to K^{(*)}\bar{K}^{(*)}$ decays which have not been measured yet. We find that the R-parity violating effects on the branching ratios and the direct CP asymmetries could be large; nevertheless their effects on the longitudinal polarizations of $B \to K^*\bar{K}^*$ decays are small. Near future experiments can test these predictions and shrink the parameter spaces.

PACS. 12.60.Jv; 12.15.Mm; 12.38.Bx; 13.25.Hw

1 Introduction

The study of exclusive hadronic B-meson decays can provide not only an interesting avenue to understand the CP-violation and flavor mixing of the quark sector in the standard model (SM), but also powerful means to probe different new physics (NP) scenarios beyond the SM. Recent experimental measurements have shown that some B decays to two light mesons deviated from the SM expectations, for example, the $\pi\pi, \pi K$ puzzle [1] and the polarization puzzle in $B \to VV$ decays [2]. Although these measurements represent quite a challenge for the theory, the SM is in no way ruled out yet, since there are many theoretical uncertainties in low energy QCD. However, it will be under considerable strain if the experimental data persist for a long time.

Among those NP models that survived the electroweak (EW) data, one of the most respectable options is the R-parity violating (RPV) supersymmetry (SUSY). The possible appearance of the RPV couplings [3], which will violate the lepton and baryon number conservation, has gained full attention in searching for SUSY [4,5]. The effect of the RPV SUSY on B decays have been extensively investigated previously in the literature [6,7], and it has been proposed as a possible resolution to the polarization puzzle and the $\pi\pi, \pi K$ puzzle [8]. The pure penguin $B \to K^{(*)}\bar{K}^{(*)}$ decays are closely related with the puzzles which are inconsistent with the SM predictions, and therefore are very important for understanding the dynamics of nonleptonic two-body B decays, which have been studied in [9]. If the RPV SUSY is the right model to resolve these puzzles, the same type of NP will affect the $B \to K^{(*)}\bar{K}^{(*)}$ decays. In this work, we shall study the RPV SUSY effects in the $B \to K^{(*)}\bar{K}^{(*)}$ decays by using the QCD factorization (QCDF) approach [10] for hadronic dynamics. The $B \to K^{(*)}\bar{K}^{(*)}$ decays are all induced at the quark level by the $b \to ds\bar{s}$ process, and they involve the same set of RPV coupling constants. Using the latest experimental data and the theoretical parameters, we obtain the new upper limits on the relevant RPV couplings. Then we use the constrained regions of parameters to examine the RPV effects on observations in the $B \to K^{(*)}\bar{K}^{(*)}$ decays which have not been measured yet.

The paper is arranged as follows. In Sect. 2, we calculate the CP averaged branching ratios, the direct CP asymmetries of $B \to K^{(*)}\bar{K}^{(*)}$ and the polarization fractions in $B \to K^*\bar{K}^*$ decays, taking account of the RPV effects with the QCDF approach. In Sect. 3, we tabulate the theoretical input in our numerical analysis. Section 4 deals with the numerical results. We display the constrained parameter spaces which satisfy all the experimental data, and then we use the constrained parameter spaces to predict the RPV effects on the other observable quantities, which have not been measured yet in the $B \to K^{(*)}\bar{K}^{(*)}$ system. Section 5 contains our summary and conclusion.

[a] e-mail: ruminwang@henannu.edu.cn
[b] e-mail: yangyd@henannu.edu.cn

2 The theoretical frame for $B \to K^{(*)}\bar{K}^{(*)}$ decays

2.1 The decay amplitudes in the SM

In the SM, the low energy effective Hamiltonian for the $\Delta B = 1$ transition at the scale μ is given by [11]

$$\mathcal{H}_{\rm eff}^{\rm SM} = \frac{G_{\rm F}}{\sqrt{2}} \sum_{p=u,c} \lambda_p \Bigg\{ C_1 Q_1^p + C_2 Q_2^p + \sum_{i=3}^{10} \Big[C_i Q_i + C_{7\gamma} Q_{7\gamma} + C_{8g} Q_{8g} \Big] \Bigg\} + \text{h.c.}\,, \quad (1)$$

where $\lambda_p = V_{pb} V_{pq}^*$ for the $b \to q$ transition ($p \in \{u, c\}, q \in \{d, s\}$), and the detailed definition of the operator base can be found in [11].

Using the weak effective Hamiltonian given by (1), we can now write the decay amplitudes for the general two-body hadronic $B \to M_1 M_2$ decays as

$$\begin{aligned} \mathcal{A}^{\rm SM}(B \to M_1 M_2) &= \langle M_1 M_2 | \mathcal{H}_{\rm eff}^{\rm SM} | B \rangle \\ &= \frac{G_{\rm F}}{\sqrt{2}} \sum_p \sum_i \lambda_p C_i(\mu) \\ &\quad \times \langle M_1 M_2 | Q_i(\mu) | B \rangle \,. \end{aligned} \quad (2)$$

The essential theoretical difficulty for obtaining the decay amplitude arises from the evaluation of the hadronic matrix elements $\langle M_1 M_2 | Q_i(\mu) | B \rangle$. There are at least three approaches with different considerations to tackle the said difficulty: the naive factorization (NF) [12, 13], the perturbative QCD [14], and the QCDF [10]. The QCDF developed by Beneke, Buchalla, Neubert and Sachrajda is a powerful framework for studying charmless B decays. We will employ the QCDF approach in this paper.

The QCDF [10] allows us to compute the nonfactorizable corrections to the hadronic matrix elements $\langle M_1 M_2 | O_i | B \rangle$ in the heavy quark limit. The decay amplitude has the form

$$\begin{aligned} \mathcal{A}^{\rm SM}(B \to M_1 M_2) &= \frac{G_{\rm F}}{\sqrt{2}} \sum_p \sum_i \lambda_p \\ &\times \Big\{ a_i^p \langle M_2 | J_2 | 0 \rangle \langle M_1 | J_1 | B \rangle + b_i^p \langle M_1 M_2 | J_2 | 0 \rangle \langle 0 | J_1 | B \rangle \Big\}, \end{aligned} \quad (3)$$

where the effective parameters a_i^p including nonfactorizable corrections at order of $\alpha_{\rm s}$. They are calculated from the vertex corrections, the hard spectator scattering, and the QCD penguin contributions, which are shown in Fig. 1. The parameters b_i^p are calculated from the weak annihilation contributions as shown in Fig. 2.

Under the naive factorization (NF) approach, the factorized matrix element is given by

$$\begin{aligned} A_{M_1 M_2} &\equiv \langle M_2 | (\bar{q}_2 \gamma_\mu (1 - \gamma_5) q_3) | 0 \rangle \\ &\quad \times \langle M_1 | \left(\bar{b} \gamma^\mu (1 - \gamma_5) q_1 \right) | B \rangle \,. \end{aligned} \quad (4)$$

In terms of the decay constant and form factors [15], the $A_{M_1 M_2}$ are expressed as

$$A_{M_1 M_2} = \begin{cases} {\rm i} f_{M_2} m_B^2 F_0^{B \to M_1}(m_{M_2}^2)\,, & \text{if } M_1 = P, M_2 = P\,, \\ f_{M_2} m_B^2 F_0^{B \to M_1}(m_{M_2}^2)\,, & \text{if } M_1 = P,\ M_2 = V\,, \\ -f_{M_2} m_B^2 A_0^{B \to M_1}(m_{M_2}^2)\,, & \text{if } M_1 = V,\ M_2 = P\,, \\ -{\rm i} f_{M_2} m_{M_2} \Big[(\varepsilon_1^* \cdot \varepsilon_2^*)(m_B + m_{M_1}) \\ \quad \times A_1^{B \to M_1}(m_{M_2}^2) - (\varepsilon_1^* \cdot p_B)(\varepsilon_2^* \cdot p_B) \\ \quad \times \frac{2 A_2^{B \to M_1}(m_{M_2}^2)}{m_B + m_{M_1}} \\ \quad + {\rm i} \epsilon_{\mu\nu\alpha\beta} \varepsilon_2^{*\mu} \varepsilon_1^{*\nu} p_B^\alpha p_1^\beta \frac{2 V^{B \to M_1}(m_{M_2}^2)}{m_B + m_{M_1}} \Big], \\ \qquad \text{if } M_1 = V,\ M_2 = V\,, \end{cases} \quad (5)$$

where $P(V)$ denote a pseudoscalar (vector) meson, $p_B(m_B)$ is the four-momentum (mass) of the B-meson, m_{M_i} are the masses of the M_i-mesons, and ε_i^* is the polarization vector of the vector mesons M_i.

Following Beneke and Neubert [16], coefficients a_i^p can be split into two parts: $a_i^p = a_{i,{\rm I}}^p + a_{i,{\rm II}}^p$. The first part contains the NF contribution and the sum of nonfactorizable vertex and penguin corrections, while the second one arises from the hard spectator scattering. The coefficients read [16]

$$\begin{aligned} a_{1,{\rm I}} &= C_1 + \frac{C_2}{N_C} \left[1 + \frac{C_F \alpha_{\rm s}}{4\pi} V_{M_2} \right], \\ a_{1,{\rm II}} &= \frac{C_2}{N_C} \frac{C_F \alpha_{\rm s}}{4\pi} H_{M_1 M_2}\,, \\ a_{2,{\rm I}} &= C_2 + \frac{C_1}{N_C} \left[1 + \frac{C_F \alpha_{\rm s}}{4\pi} V_{M_2} \right], \\ a_{2,{\rm II}} &= \frac{C_1}{N_C} \frac{C_F \alpha_{\rm s}}{4\pi} H_{M_1 M_2}\,, \\ a_{3,{\rm I}} &= C_3 + \frac{C_4}{N_C} \left[1 + \frac{C_F \alpha_{\rm s}}{4\pi} V_{M_2} \right], \\ a_{3,{\rm II}} &= \frac{C_4}{N_C} \frac{C_F \alpha_{\rm s}}{4\pi} H_{M_1 M_2}\,, \\ a_{4,{\rm I}}^p &= C_4 + \frac{C_3}{N_C} \left[1 + \frac{C_F \alpha_{\rm s}}{4\pi} V_{M_2} \right] + \frac{C_F \alpha_{\rm s}}{4\pi} \frac{P_{M_2,2}^p}{N_C}\,, \\ a_{4,{\rm II}} &= \frac{C_3}{N_C} \frac{C_F \alpha_{\rm s}}{4\pi} H_{M_1 M_2}\,, \\ a_{5,{\rm I}} &= C_5 + \frac{C_6}{N_C} \left[1 + \frac{C_F \alpha_{\rm s}}{4\pi} (-12 - V_{M_2}) \right], \\ a_{5,{\rm II}} &= \frac{C_6}{N_C} \frac{C_F \alpha_{\rm s}}{4\pi} (-H_{M_1 M_2})\,, \\ a_{6,{\rm I}}^p &= \left\{ C_6 + \frac{C_5}{N_C} \left[1 - 6 \frac{C_F \alpha_{\rm s}}{4\pi} \right] \right\} N_{M_2} + \frac{C_F \alpha_{\rm s}}{4\pi} \frac{P_{M_2,3}^p}{N_C}\,, \\ a_{6,{\rm II}} &= 0, \\ a_{7,{\rm I}} &= C_7 + \frac{C_8}{N_C} \left[1 + \frac{C_F \alpha_{\rm s}}{4\pi} (-12 - V_{M_2}) \right], \\ a_{7,{\rm II}} &= \frac{C_8}{N_C} \frac{C_F \alpha_{\rm s}}{4\pi} (-H_{M_1 M_2})\,, \\ a_{8,{\rm I}}^p &= \left\{ C_8 + \frac{C_7}{N_C} \left[1 - 6 \frac{C_F \alpha_{\rm s}}{4\pi} \right] \right\} N_{M_2} + \frac{\alpha_e}{9\pi} \frac{P_{M_2,3}^{p,{\rm EW}}}{N_C}\,, \end{aligned}$$

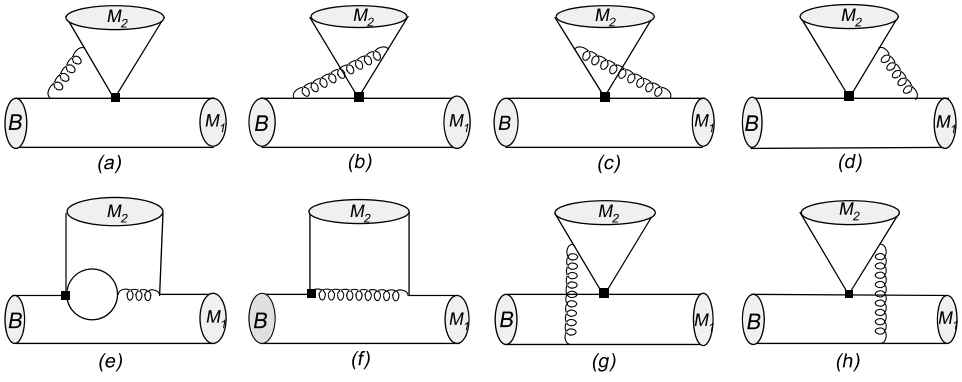

Fig. 1. The next to leading order nonfactorizable contributions to the coefficients a_i^p

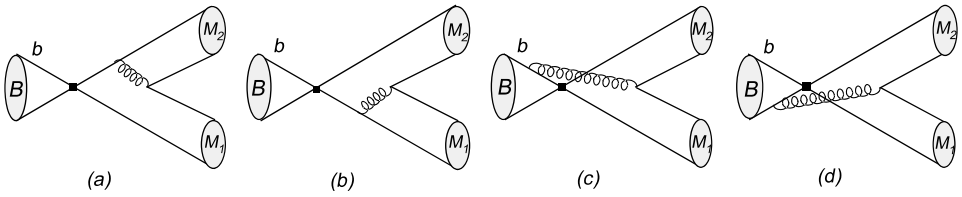

Fig. 2. The weak annihilation contributions to the coefficients b_i^p

$$
\begin{aligned}
a_{8,\mathrm{II}} &= 0\,,\\
a_{9,\mathrm{I}} &= C_9 + \frac{C_{10}}{N_C}\left[1+\frac{C_F\alpha_\mathrm{s}}{4\pi}V_{M_2}\right]\,,\\
a_{9,\mathrm{II}} &= \frac{C_{10}}{N_C}\frac{C_F\alpha_\mathrm{s}}{4\pi}H_{M_1M_2}\,,\\
a^p_{10,\mathrm{I}} &= C_{10} + \frac{C_9}{N_C}\left[1+\frac{C_F\alpha_\mathrm{s}}{4\pi}V_{M_2}\right] + \frac{\alpha_e}{9\pi}\frac{P^{p,\mathrm{EW}}_{M_2,2}}{N_C}\,,\\
a_{10,\mathrm{II}} &= \frac{C_9}{N_C}\frac{C_F\alpha_\mathrm{s}}{4\pi}H_{M_1M_2}\,,
\end{aligned}
\tag{6}
$$

where $\alpha_\mathrm{s}\equiv\alpha_\mathrm{s}(\mu)$, $C_F=(N_C^2-1)/(2N_C)$, $N_C=3$ is the number of colors, and $N_{M_2}=1(0)$ for M_2 is a pseudoscalar (vector) meson. The quantities $V_{M_2}, H_{M_1M_2}$, $P^p_{M_2,2}, P^p_{M_2,3}$, $P^{p,\mathrm{EW}}_{M_2,2}$ and $P^{p,\mathrm{EW}}_{M_2,3}$ consist of convolutions of hard-scattering kernels with meson distribution amplitudes. Specifically, the terms V_{M_2} come from the vertex corrections in Fig. 1a–d, $P^p_{M_2,2}$ and $P^p_{M_2,3}$ ($P^{p,\mathrm{EW}}_{M_2,2}$ and $P^{p,\mathrm{EW}}_{M_2,3}$) arise from QCD (EW) penguin contractions and the contributions from the dipole operators as depicted by Fig. 1e and f. $H_{M_1M_2}$ is due to the hard spectator scattering as Fig. 1g and h. For the penguin terms, the subscript 2 and 3 indicate the twist-2 and -3 distribution amplitudes of light mesons, respectively. Explicit forms for these quantities are relegated to Appendix A.

We use the convention that M_1 contains an antiquark from the weak vertex, for the non-singlet annihilation M_2 then contains a quark from the weak vertex. The parameters $b_i^p\equiv b_i^p(M_1,M_2)$ in(3) correspond to the weak annihilation contributions and are given as [17]

$$
\begin{aligned}
b_1(M_1,M_2) &= \frac{C_F}{N_C^2}C_1A_1^i(M_1,M_2)\,,\\
b_2(M_1,M_2) &= \frac{C_F}{N_C^2}C_2A_1^i(M_1,M_2)\,,
\end{aligned}
$$

$$
\begin{aligned}
b_3^p(M_1,M_2) &= \frac{C_F}{N_C^2}\Big[C_3A_1^i(M_1,M_2)\\
&\quad + C_5\left(A_3^i(M_1,M_2)+A_3^f(M_1,M_2)\right)\\
&\quad + N_CC_6A_3^f(M_1,M_2)\Big]\,,\\
b_4^p(M_1,M_2) &= \frac{C_F}{N_C^2}\left[C_4A_1^i(M_1,M_2)+C_6A_2^i(M_1,M_2)\right]\,,\\
b_3^{p,\mathrm{EW}}(M_1,M_2) &= \frac{C_F}{N_C^2}\Big[C_9A_1^i(M_1,M_2)\\
&\quad + C_7\left(A_3^i(M_1,M_2)+A_3^f(M_1,M_2)\right)\\
&\quad + N_CC_8A_3^f(M_1,M_2)\Big]\,,\\
b_4^{p,\mathrm{EW}}(M_1,M_2) &= \frac{C_F}{N_C^2}\Big[C_{10}A_1^i(M_1,M_2)\\
&\quad + C_8A_2^i(M_1,M_2)\Big]\,,
\end{aligned}
\tag{7}
$$

the annihilation coefficients (b_1,b_2), (b_3^p,b_4^p) and $(b_3^{p,\mathrm{EW}}, b_4^{p,\mathrm{EW}})$ correspond to the contributions of the tree, QCD penguins and EW penguins operators insertions, respectively. The explicit form for the building blocks $A_k^{i,f}(M_1,M_2)$ can be found in Appendix A.

With the coefficients in (6) and (7), we can obtain the decay amplitudes of the SM part $\mathcal{A}_f^{\mathrm{SM}}$ (the subscript "f" denotes the part without the contribution from the annihilation part) and $\mathcal{A}_a^{\mathrm{SM}}$ (the subscript "a" denotes the annihilation part). The SM part amplitudes of $B\to K^{(*)}\bar{K}^{(*)}$ decays are given in Appendix B.

2.2 R-parity violating SUSY effects in the decays

In the most general superpotential of the minimal supersymmetric standard model (MSSM), the RPV superpoten-

tial is given by [18]

$$\mathcal{W}_{\not R_p} = \mu_i \hat{L}_i \hat{H}_u + \frac{1}{2}\lambda_{[ij]k}\hat{L}_i\hat{L}_j\hat{E}^{\rm c}_k + \lambda'_{ijk}\hat{L}_i\hat{Q}_j\hat{D}^{\rm c}_k + \frac{1}{2}\lambda''_{i[jk]}\hat{U}^{\rm c}_i\hat{D}^{\rm c}_j\hat{D}^{\rm c}_k\,, \quad (8)$$

where $\hat{L}$ and $\hat{Q}$ are the $SU(2)$-doublet lepton and quark superfields and $\hat{E}^{\rm c}$, $\hat{U}^{\rm c}$ and $\hat{D}^{\rm c}$ are the singlet superfields, while i, j and k are generation indices, and c denotes a charge conjugate field.

The bilinear RPV superpotential terms $\mu_i\hat{L}_i\hat{H}_u$ can be rotated away by suitably redefining the lepton and Higgs superfields [19]. However, the rotation will generate a soft SUSY breaking bilinear term which would affect our calculation through the penguin level. However, the processes discussed in this paper could be induced by tree-level RPV couplings, so that we would neglect sub-leading RPV penguin contributions in this study.

The λ and λ' couplings in (8) break the lepton number, while the λ'' couplings break the baryon number conservation. There are 27 λ'_{ijk} couplings, 9 λ_{ijk} and 9 λ''_{ijk} couplings. $\lambda_{[ij]k}$ are antisymmetric with respect to their first two indices, and $\lambda''_{i[jk]}$ are antisymmetric with j and k. The antisymmetry of the baryon number violating couplings $\lambda''_{i[jk]}$ in the last two indices implies that there are no λ''_{ijk} operator generating the $\bar{b} \to \bar{s}s\bar{s}$ and $\bar{b} \to \bar{d}d\bar{d}$ transitions.

From (8), we can obtain the following four fermion effective Hamiltonian due to the sleptons exchange as shown in Fig. 3:

$$\mathcal{H}^{\not R_p}_{2u-2d} = \sum_i \frac{\lambda'_{ijm}\lambda'^*_{ikl}}{2m^2_{\tilde{e}_{{\rm L}i}}}\eta^{-8/\beta_0}(\bar{d}_m\gamma^\mu P_{\rm R}d_l)_8(\bar{u}_k\gamma_\mu P_{\rm L}u_j)_8\,,$$
$$\mathcal{H}^{\not R_p}_{4d} = \sum_i \frac{\lambda'_{ijm}\lambda'^*_{ikl}}{2m^2_{\tilde{\nu}_{{\rm L}i}}}\eta^{-8/\beta_0}(\bar{d}_m\gamma^\mu P_{\rm R}d_l)_8(\bar{d}_k\gamma_\mu P_{\rm L}d_j)_8\,. \quad (9)$$

The four fermion effective Hamiltonian due to the squarks exchanging as shown in Fig. 4 are

$$\mathcal{H}'^{\not R_p}_{2u-2d} = \sum_n \frac{\lambda''_{ikn}\lambda''^*_{jln}}{2m^2_{\tilde{d}_n}}\eta^{-4/\beta_0}\left\{\left[(\bar{u}_i\gamma^\mu P_{\rm R}u_j)_1(\bar{d}_k\gamma_\mu P_{\rm R}d_l)_1 - (\bar{u}_i\gamma^\mu P_{\rm R}u_j)_8(\bar{d}_k\gamma_\mu P_{\rm R}d_l)_8\right] - \left[(\bar{d}_k\gamma^\mu P_{\rm R}u_j)_1(\bar{u}_i\gamma_\mu P_{\rm R}d_l)_1 - (\bar{d}_k\gamma^\mu P_{\rm R}u_j)_8(\bar{u}_i\gamma_\mu P_{\rm R}d_l)_8\right]\right\}\,,$$

$$\mathcal{H}'^{\not R_p}_{4d} = \sum_n \frac{\lambda''_{nik}\lambda''^*_{njl}}{4m^2_{\tilde{u}_n}}\eta^{-4/\beta_0}\left[(\bar{d}_i\gamma^\mu P_{\rm R}d_j)_1(\bar{d}_k\gamma_\mu P_{\rm R}d_l)_1 - (\bar{d}_i\gamma^\mu P_{\rm R}d_j)_8(\bar{d}_k\gamma_\mu P_{\rm R}d_l)_8\right]\,. \quad (10)$$

In (9) and (10), $P_{\rm L} = \frac{1-\gamma_5}{2}$, $P_{\rm R} = \frac{1+\gamma_5}{2}$, $\eta = \frac{\alpha_{\rm s}(m_{\tilde{f}})}{\alpha_{\rm s}(m_b)}$ and $\beta_0 = 11 - \frac{2}{3}n_f$. The subscript for the currents $(j_\mu)_{1,8}$ represents the current in the color singlet and octet, respectively. The coefficients η^{-4/β_0} and η^{-8/β_0} are due to the running from the sfermion mass scale $m_{\tilde{f}}$ (100 GeV assumed) down to the m_b scale. Since it is always assumed in phenomenology for numerical display that only one sfermion contributes at one time, we neglect the mixing between the operators when we use the renormalization group equation (RGE) to run $\mathcal{H}^{\not R_p}_{\rm eff}$ down to the low scale.

The RPV amplitude for the decays can be written as

$$\mathcal{A}^{\not R_p}(B \to M_1M_2) = \left\langle M_1M_2|\mathcal{H}^{\not R_p}_{\rm eff}|B\right\rangle\,. \quad (11)$$

The product RPV couplings can in general be complex and their phases may induce new contribution to CP-violation, which we write as

$$\Lambda_{ijk}\Lambda^*_{lmn} = |\Lambda_{ijk}\Lambda_{lmn}|\,{\rm e}^{{\rm i}\phi_{\not R_p}}\,,$$
$$\Lambda^*_{ijk}\Lambda_{lmn} = |\Lambda_{ijk}\Lambda_{lmn}|\,{\rm e}^{-{\rm i}\phi_{\not R_p}}\,, \quad (12)$$

here the RPV coupling constant $\Lambda \in \{\lambda, \lambda', \lambda''\}$, and $\phi_{\not R_p}$ is the RPV weak phase, which may be any value between $-\pi$ and π.

For simplicity we only consider the vertex corrections and the hard spectator scattering in the RPV decay amplitudes. We ignore the RPV penguin contributions, which are expected to be small even compared with the SM penguin amplitudes; this follows from the smallness of the relevant RPV couplings compared with the SM gauge couplings. The bounds on the RPV couplings are insensitive to the inclusion of the RPV penguins [20]. We also neglected the annihilation contributions in the RPV amplitudes. The R-parity violating part of the decay amplitudes $\mathcal{A}^{\not R_p}$ can be found in Appendix C.

2.3 The total decay amplitude

With the QCDF, we can get the total decay amplitude:

$$\mathcal{A}(B \to M_1M_2) = \mathcal{A}^{\rm SM}_f(B \to M_1M_2) + \mathcal{A}^{\rm SM}_a(B \to M_1M_2) + \mathcal{A}^{\not R_p}(B \to M_1M_2)\,. \quad (13)$$

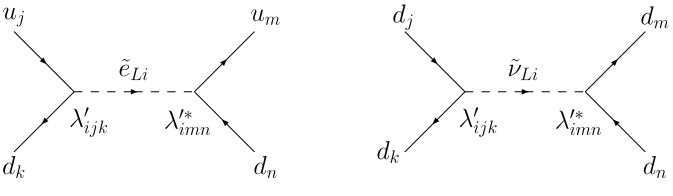

Fig. 3. Sleptons exchanging diagrams for nonleptonic B decays

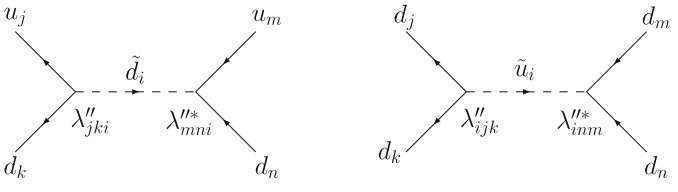

Fig. 4. Squarks exchanging diagrams for nonleptonic B decays

The expressions for the SM amplitude $\mathcal{A}_{f,a}^{\rm SM}$ and the RPV amplitude $\mathcal{A}^{\not R_p}$ are presented in Appendices B and C, respectively. From the amplitude in (13), the branching ratio reads

$$\mathcal{B}(B \to M_1 M_2) = \frac{\tau_B |p_{\rm c}|}{8\pi m_B^2} \left|\mathcal{A}(B \to M_1 M_2)\right|^2 S\,, \quad (14)$$

where $S = 1/2$ if M_1 and M_2 are identical, and $S = 1$ otherwise; τ_B is the B lifetime, $|p_{\rm c}|$ is the center of mass momentum in the center of mass frame of the B-meson and given by

$$|p_{\rm c}| = \frac{1}{2m_B} \times \sqrt{\left[m_B^2 - (m_{M_1} + m_{M_2})^2\right]\left[m_B^2 - (m_{M_1} - m_{M_2})^2\right]}\,. \quad (15)$$

The direct CP asymmetry is defined as

$$\mathcal{A}_{CP}^{\rm dir} = \frac{\mathcal{B}(\bar{B} \to \bar{f}) - \mathcal{B}(B \to f)}{\mathcal{B}(\bar{B} \to \bar{f}) + \mathcal{B}(B \to f)}\,. \quad (16)$$

In the $B \to VV$ decay, the longitudinal polarization fraction is defined by

$$f_{\rm L} = \frac{\Gamma_{\rm L}}{\Gamma} = \frac{|\mathcal{A}_0|^2}{|\mathcal{A}_0|^2 + |\mathcal{A}_+|^2 + |\mathcal{A}_-|^2}\,, \quad (17)$$

where $A_0(A_\pm)$ corresponding to the longitudinal(two transverse) polarization amplitude(s) for $B \to VV$ decay.

3 Input parameters

3.1 Wilson coefficients

We use the next-to-leading Wilson coefficients calculated in the naive dimensional regularization (NDR) scheme at m_b scale [11]:

$$\begin{aligned} C_1 = 1.082\,, \quad C_2 = -0.185\,, \quad C_3 = 0.014\,, \\ C_4 = -0.035\,, \quad C_5 = 0.009\,, \quad C_6 = -0.041\,, \\ C_7/\alpha_e = -0.002\,, \quad C_8/\alpha_e = 0.054\,, \quad C_9/\alpha_e = -1.292\,, \\ C_{10}/\alpha_e = 0.263\,, \quad C_{7\gamma}^{\rm eff} = -0.299\,, \quad C_{8g}^{\rm eff} = -0.143\,. \end{aligned} \quad (18)$$

3.2 The CKM matrix element

The magnitude of the CKM elements are taken from [21]:

$$\begin{aligned} &|V_{ud}| = 0.9738 \pm 0.0005\,, && |V_{us}| = 0.2200 \pm 0.0026\,, \\ &|V_{ub}| = 0.00367 \pm 0.00047\,, && |V_{cd}| = -0.224 \pm 0.012\,, \\ &|V_{cs}| = 0.996 \pm 0.013\,, && |V_{cb}| = 0.0413 \pm 0.0015\,, \\ &|V_{tb}^* V_{td}| = 0.0083 \pm 0.0016\,, && |V_{tb} V_{ts}^*| = -0.047 \pm 0.008\,, \end{aligned} \quad (19)$$

and the CKM phase $\gamma = 60^\circ \pm 14^\circ$, $\sin(2\beta) = 0.736 \pm 0.049$.

3.3 Masses and lifetime

There are two types of quark mass in our analysis. One type is the pole mass which appears in the loop integration. Here we fix them as

$$m_u = m_d = m_s = 0\,, \quad m_c = 1.47\,{\rm GeV}\,, \quad m_b = 4.8\,{\rm GeV}\,. \quad (20)$$

The other type quark mass appears in the hadronic matrix elements and the chirally enhanced factor $r_\chi^P = \frac{2\mu_p}{\overline{m}_b}$ through the equations of motion. They are renormalization scale dependent. We shall use the 2004 Particle Data Group data [21] for discussion:

$$\begin{aligned} \overline{m}_u(2\,{\rm GeV}) &= 0.0015 \sim 0.004\,{\rm GeV}\,, \\ \overline{m}_d(2\,{\rm GeV}) &= 0.004 \sim 0.008\,{\rm GeV}\,, \\ \overline{m}_s(2\,{\rm GeV}) &= 0.08 \sim 0.13\,{\rm GeV}\,, \\ \overline{m}_b(\overline{m}_b) &= 4.1 \sim 4.4\,{\rm GeV}\,, \end{aligned} \quad (21)$$

and then employ the formulae in [11]:

$$\overline{m}(\mu) = \overline{m}(\mu_0)\left[\frac{\alpha_{\rm s}(\mu)}{\alpha_{\rm s}(\mu_0)}\right]^{\frac{\gamma_m^{(0)}}{2\beta_0}} \times \left[1 + \left(\frac{\gamma_m^{(1)}}{2\beta_0} - \frac{\beta_1 \gamma_m^{(0)}}{2\beta_0^2}\right)\frac{\alpha_{\rm s}(\mu) - \alpha_{\rm s}(\mu_0)}{4\pi}\right]\,, \quad (22)$$

to obtain the current quark masses to any scale. The definitions of $\gamma_m^{(0)}, \gamma_m^{(1)}, \beta_0, \beta_1$ can be found in [11].

To compute the branching ratio, the masses of the mesons are also taken from [21]:

$$\begin{aligned} m_{B_u} = 5.279\,{\rm GeV}\,, \quad m_{K^{*\pm}} = 0.892\,{\rm GeV}\,, \\ m_{K^\pm} = 0.494\,{\rm GeV}\,, \quad m_{B_d} = 5.279\,{\rm GeV}\,, \\ m_{K^{*0}} = 0.896\,{\rm GeV}\,, \quad m_{K^0} = 0.498\,{\rm GeV}\,. \end{aligned}$$

The lifetime of the B-mesons are [21]

$$\tau_{B_u} = (1.638 \pm 0.011)\,{\rm ps}\,, \quad \tau_{B_d} = (1.532 \pm 0.009)\,{\rm ps}\,. \quad (23)$$

3.4 The LCDAs of the meson

For the LCDAs of the meson, we use the asymptotic form [22–24]

$$\Phi_P(x) = 6x(1-x)\,, \quad \Phi_p^P(x) = 1\,, \quad (24)$$

for the pseudoscalar meson, and

$$\begin{aligned} \Phi_\parallel^V(x) = \Phi_\perp^V(x) = g_\perp^{(a)V} = 6x(1-x)\,, \\ g_\perp^{(v)V}(x) = \frac{3}{4}[1 + (2x-1)^2]\,, \end{aligned} \quad (25)$$

for the vector meson.

We adopt the moments of the $\Phi_1^B(\xi)$ defined in [10, 17] for our numerical evaluation:

$$\int_0^1 \mathrm{d}\xi \frac{\Phi_1^B(\xi)}{\xi} = \frac{m_B}{\lambda_B}\,, \tag{26}$$

with $\lambda_B = (0.46 \pm 0.11)\,\mathrm{GeV}$ [25]. The quantity λ_B parameterizes our ignorance about the B-meson distribution amplitudes and thus brings about considerable theoretical uncertainty.

3.5 The decay constants and form factors

For the decay constants, we take the latest light-cone QCD sum rule results (LCSR) [15] in our calculations:

$$\begin{aligned} f_{B_{u(d)}} &= 0.161\,\mathrm{GeV}\,, \quad f_K = 0.160\,\mathrm{GeV}\,, \\ f_{K^*} &= 0.217\,\mathrm{GeV}\,, \quad f_{K^*}^{\perp} = 0.156\,\mathrm{GeV}\,. \end{aligned} \tag{27}$$

For the form factors involving the $B \to K^{(*)}$ transition, we adopt the values given by [15]

$$\begin{aligned} A_0^{B_{u(d)}\to K^*}(0) &= 0.374 \pm 0.034\,, \\ A_1^{B_{u(d)}\to K^*}(0) &= 0.292 \pm 0.028\,, \\ A_2^{B_{u(d)}\to K^*}(0) &= 0.259 \pm 0.027\,, \\ V^{B_{u(d)}\to K^*}(0) &= 0.411 \pm 0.033\,, \\ F_0^{B_{u(d)}\to K}(0) &= 0.331 \pm 0.041\,. \end{aligned} \tag{28}$$

4 Numerical results and analysis

First, we will show our estimations in the SM by taking the center value of the input parameters and compare with the relevant experimental data. Then we will consider the RPV effects to constrain the relevant RPV couplings from the experimental data. Using the constrained parameter spaces, we will give the RPV SUSY predictions for the branching ratios, the direct CP asymmetries, and the longitudinal polarizations, which have not been measured yet in the $B \to K^{(*)}\bar{K}^{(*)}$ system.

When considering the RPV effects, we will use the input parameters and the experimental data which are varied randomly within 1σ variance. In the SM, the weak phase γ is well constrained; however, with the presence of the RPV, this constraint may be relaxed. We would not take γ within the SM range, but vary it randomly in the range of 0 to π to obtain conservative limits on RPV couplings. We assume that only one sfermion contributes at one time with a mass of 100 GeV. As for the other values of the sfermion masses, the bounds on the couplings in this paper can be easily obtained by scaling them with a factor $\tilde{f}^2 \equiv \left(\frac{m_{\tilde{f}}}{100\ \mathrm{GeV}}\right)^2$.

For the $B \to K^{(*)}\bar{K}^{(*)}$ modes, several branching ratios and one direct CP asymmetry have been measured by BABAR, Belle and CLEO [21, 26], and their averaged values [27] are

$$\begin{aligned} \mathcal{B}(B_u^+ \to K^+\bar{K}^0) &= (1.2 \pm 0.3) \times 10^{-6}\,, \\ \mathcal{B}(B_d^0 \to K^0\bar{K}^0) &= (0.96^{+0.25}_{-0.24}) \times 10^{-6}\,, \\ \mathcal{B}(B_u^+ \to K^+\bar{K}^{*0}) &< 5.3 \times 10^{-6} \quad (\,90\%\ \mathrm{CL}\,)\,, \\ \mathcal{B}(B_u^+ \to K^{*+}\bar{K}^{*0}) &< 71 \times 10^{-6} \quad (\,90\%\ \mathrm{CL}\,)\,, \\ \mathcal{B}(B_d^0 \to K^{*0}\bar{K}^{*0}) &< 22 \times 10^{-6} \quad (\,90\%\ \mathrm{CL}\,)\,, \\ \mathcal{A}_{CP}^{\mathrm{dir}}(B_u^+ \to K^+\bar{K}^0) &= 0.15 \pm 0.33\,. \end{aligned} \tag{29}$$

The numerical results in the SM are presented in Table 1, which shows the results for the CP averaged branching ratios ($\mathcal{B}$), the direct CP asymmetries ($\mathcal{A}_{CP}^{\mathrm{dir}}$) and the longitudinal polarization fractions (f_{L}).

From Table 1, we can see that the branching ratios for them are expected to be quite small, of order 10^{-7}, since $B \to K^{(*)}\bar{K}^{(*)}$ are the pure $b \to d$ penguin dominated decays. The subleading diagrams may lead to significant CP-violations in most $B \to K^{(*)}\bar{K}^{(*)}$ decays. As $B_d^0 \to K^{\pm}K^{\mp}$ decays involved only nonfactorizable annihilation contributions, their branching ratios are much smaller than those of the $B \to K^+\bar{K}^0, K^0\bar{K}^0$ decays, and we would not study the $B_d^0 \to K^{\pm}K^{\mp}$ modes in this paper. It should be noted that the amplitude for $\bar{B}_d^0 \to K^0\bar{K}^{*0}$ is not simply re-

Table 1. The SM predictions for $\mathcal{B}$ (in unit of 10^{-6}), $\mathcal{A}_{CP}^{\mathrm{dir}}$ and f_{L} in $B \to K^{(*)}\bar{K}^{(*)}$ decays in the framework of NF and QCDF

Decays	$\mathcal{B}$		$\mathcal{A}_{CP}^{\mathrm{dir}}$		f_{L}	
	NF	QCDF	NF	QCDF	NF	QCDF
$B_u^+ \to K^+\bar{K}^0$	0.61	0.89	0.00	−0.13		
$B_d^0 \to K^0\bar{K}^0$	0.57	0.89	0.00	−0.13		
$B_u^+ \to K^{*+}\bar{K}^0$	0.06	0.10	0.00	−0.19		
$B_u^+ \to K^+\bar{K}^{*0}$	0.15	0.18	0.00	−0.08		
$B_d^0 \to K^{*0}\bar{K}^0$	0.05	0.10	0.00	−0.18		
$B_d^0 \to K^0\bar{K}^{*0}$	0.14	0.16	0.00	−0.10		
$B_u^+ \to K^{*+}\bar{K}^{*0}$	0.20	0.22	0.00	−0.22	0.91	0.90
$B_d^0 \to K^{*0}\bar{K}^{*0}$	0.19	0.20	0.00	−0.22	0.91	0.90

lated to that for $B_d^0 \to K^0\bar{K}^{*0}$ since the spectator quark is part of the K^0 in the latter decay, while in the former of the $\bar{K}^{*0}$.

Although recent experimental results in $B \to K^{(*)}\bar{K}^{(*)}$ seem to be roughly consistent with the SM predictions, there are still windows for NP in these processes. We now

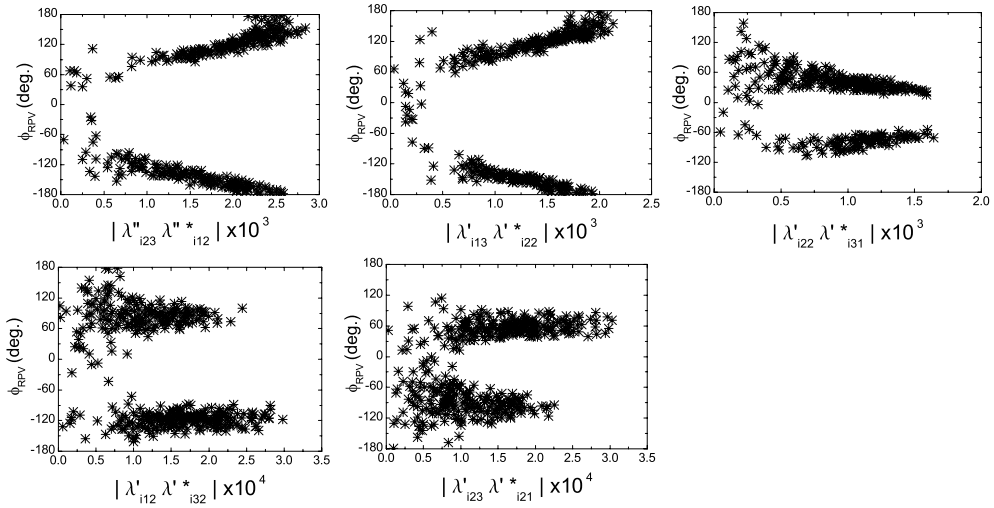

Fig. 5. The allowed parameter spaces for the relevant RPV couplings constrained by $B \to K^{(*)}\bar{K}^{(*)}$, and $\phi_{\rm RPV}$ denotes the RPV weak phase

Table 2. Bounds for the relevant RPV couplings by $B \to K^{(*)}\bar{K}^{(*)}$ decays for 100 GeV sfermions, and previous bounds are listed for comparison

Couplings	Bounds [process]	Previous bounds [process]
$\lvert\lambda''_{i23}\lambda''^{*}_{i12}\rvert$	$\le 2.9\times10^{-3}\ \left[B \to K^{(*)}\bar{K}^{(*)}\right]$	$\le 5\times10^{-3}[B\to K\bar{K}]$ $\le 6\times10^{-5}[B^0\to\phi\pi^0,\phi\phi]$ [4]
$\lvert\lambda'_{i13}\lambda'^{*}_{i22}\rvert$	$\le 2.2\times10^{-3}\ \left[B \to K^{(*)}\bar{K}^{(*)}\right]$	$\le 2.9\times10^{-3}\ [B \to K\bar{K}]$ [7]
$\lvert\lambda'_{i22}\lambda'^{*}_{i31}\rvert$	$\le 1.7\times10^{-3}\ \left[B \to K^{(*)}\bar{K}^{(*)}\right]$	$\le 1\times10^{-4}\ \ [K\bar{K}]$ [4]
$\lvert\lambda'_{i12}\lambda'^{*}_{i32}\rvert$	$\le 3.0\times10^{-4}\ \left[B \to K\bar{K}^{(*)}, \bar{K}K^{(*)}\right]$	$\le 4\times10^{-4}\ \left[B^0 \to \phi\pi^0\right]$ [4]
$\lvert\lambda'_{i23}\lambda'^{*}_{i21}\rvert$	$\le 3.0\times10^{-4}\ \left[B \to K\bar{K}^{(*)}, \bar{K}K^{(*)}\right]$	$\le 4\times10^{-4}\ \left[B^0 \to \phi\pi^0\right]$ [4]

Table 3. The theoretical predictions for $\mathcal{B}$ (in unit of 10^{-6}), $\mathcal{A}_{CP}^{\rm dir}$ and $f_{\rm L}$ base on the RPV SUSY model, which are obtained by the allowed regions of the different RPV couplings

	$\lambda''_{i23}\lambda''^{*}_{i12}$	$\lambda'_{i13}\lambda'^{*}_{i22}$	$\lambda'_{i22}\lambda'^{*}_{i31}$	$\lambda'_{i12}\lambda'^{*}_{i32}$	$\lambda'_{i23}\lambda'^{*}_{i21}$
$\mathcal{B}(B_u^+ \to K^{*+}\bar{K}^0)$	$[0.0052, 7.8]$	$[0.013, 5.5]$	$[0.0059, 6.4]$	$[0.056, 1.4]$	$[0.064, 1.3]$
$\mathcal{B}(B_u^+ \to K^+\bar{K}^{*0})$	$[0.071, 5.3]$	$[0.056, 5.3]$	$[0.0096, 5.3]$		
$\mathcal{B}(B_d^0 \to K^{*0}\bar{K}^0)$	$[0.0060, 7.5]$	$[0.011, 5.1]$	$[0.0053, 6.1]$	$[0.049, 1.5]$	$[0.054, 1.2]$
$\mathcal{B}(B_d^0 \to K^0\bar{K}^{*0})$	$[0.069, 5.0]$	$[0.050, 5.1]$	$[0.0093, 5.0]$		
$\mathcal{B}(B_u^+ \to K^{*+}\bar{K}^{*0})$	$[0.087, 19]$	$[0.041, 23]$	$[0.029, 16]$		
$\mathcal{B}(B_d^0 \to K^{*0}\bar{K}^{*0})$	$[0.080, 17]$	$[0.039, 22]$	$[0.027, 15]$		
$\mathcal{A}_{CP}^{\rm dir}(B_d^0 \to K^0\bar{K}^0)$	$[-0.75, 0.57]$	$[-0.19, 0.44]$	$[-0.18, 0.47]$	$[-0.18, 0.47]$	$[-0.18, 0.50]$
$\mathcal{A}_{CP}^{\rm dir}(B_u^+ \to K^{*+}\bar{K}^0)$	$[-0.19, 0.17]$	$[-0.32, 0.17]$	$[-0.42, 0.47]$	$[-0.99, 0.99]$	$[-0.98, 0.76]$
$\mathcal{A}_{CP}^{\rm dir}(B_u^+ \to K^+\bar{K}^{*0})$	$[-0.63, 0.63]$	$[-0.38, 0.47]$	$[-0.65, 0.38]$		
$\mathcal{A}_{CP}^{\rm dir}(B_d^0 \to K^{*0}\bar{K}^0)$	$[-0.28, 0.19]$	$[-0.33, 0.17]$	$[-0.28, 0.80]$	$[-0.99, 0.99]$	$[-0.99, 0.73]$
$\mathcal{A}_{CP}^{\rm dir}(B_d^0 \to K^0\bar{K}^{*0})$	$[-0.76, 0.62]$	$[-0.38, 0.48]$	$[-0.39, 0.40]$		
$\mathcal{A}_{CP}^{\rm dir}(B_u^+ \to K^{*+}\bar{K}^{*0})$	$[-0.63, 0.30]$	$[-0.26, 0.25]$	$[-0.77, 0.32]$		
$\mathcal{A}_{CP}^{\rm dir}(B_d^0 \to K^{*0}\bar{K}^{*0})$	$[-0.46, 0.38]$	$[-0.26, 0.25]$	$[-0.77, 0.32]$		
$f_L(B_u^+ \to K^{*+}\bar{K}^{*0})$	$[0.72, 0.97]$	$[0.59, 0.95]$	$[0.74, 0.93]$		
$f_L(B_d^0 \to K^{*0}\bar{K}^{*0})$	$[0.72, 0.97]$	$[0.59, 0.95]$	$[0.74, 0.93]$		

turn to the RPV effects in $B \to K^{(*)}\bar{K}^{(*)}$ decays. There are five RPV coupling constants contributing to the eight $B \to K^{(*)}\bar{K}^{(*)}$ decay modes. We use $\mathcal{B}$, $\mathcal{A}_{CP}^{\rm dir}$ and the experimental constraints shown in (29) to constrain the relevant RPV parameters. As known, data on low energy processes can be used to impose rather strict constraints on many of these couplings. In Fig. 5, we present the bounds on the RPV couplings. The random variation of the parameters subjected to the constraints as discussed above leads to the scatter plots displayed in Fig. 5.

From Fig. 5, we find that every RPV weak phase has two possible bands; one band is for a positive value of the RPV weak phase, and another for the negative one. We also find that the magnitudes of the relevant RPV couplings have been upper limited. The upper limits are summarized in Table 2. For comparison, the existing bounds on these quadric coupling products [4, 7] are also listed. Our bounds on $|\lambda'_{i13}\lambda'^{*}_{i22}|$, $|\lambda'_{i12}\lambda'^{*}_{i32}|$ and $|\lambda'_{i23}\lambda'^{*}_{i21}|$ are stronger than the existing ones.

Using the constrained parameter spaces shown in Fig. 5, one can predict the RPV effects on the other quantities which have not been measured yet in $B \to K^{(*)}\bar{K}^{(*)}$ decays. With the expressions for $\mathcal{B}$, $\mathcal{A}_{CP}^{\rm dir}$ and $f_{\rm L}$ at hand, we perform a scan on the input parameters and the new con-

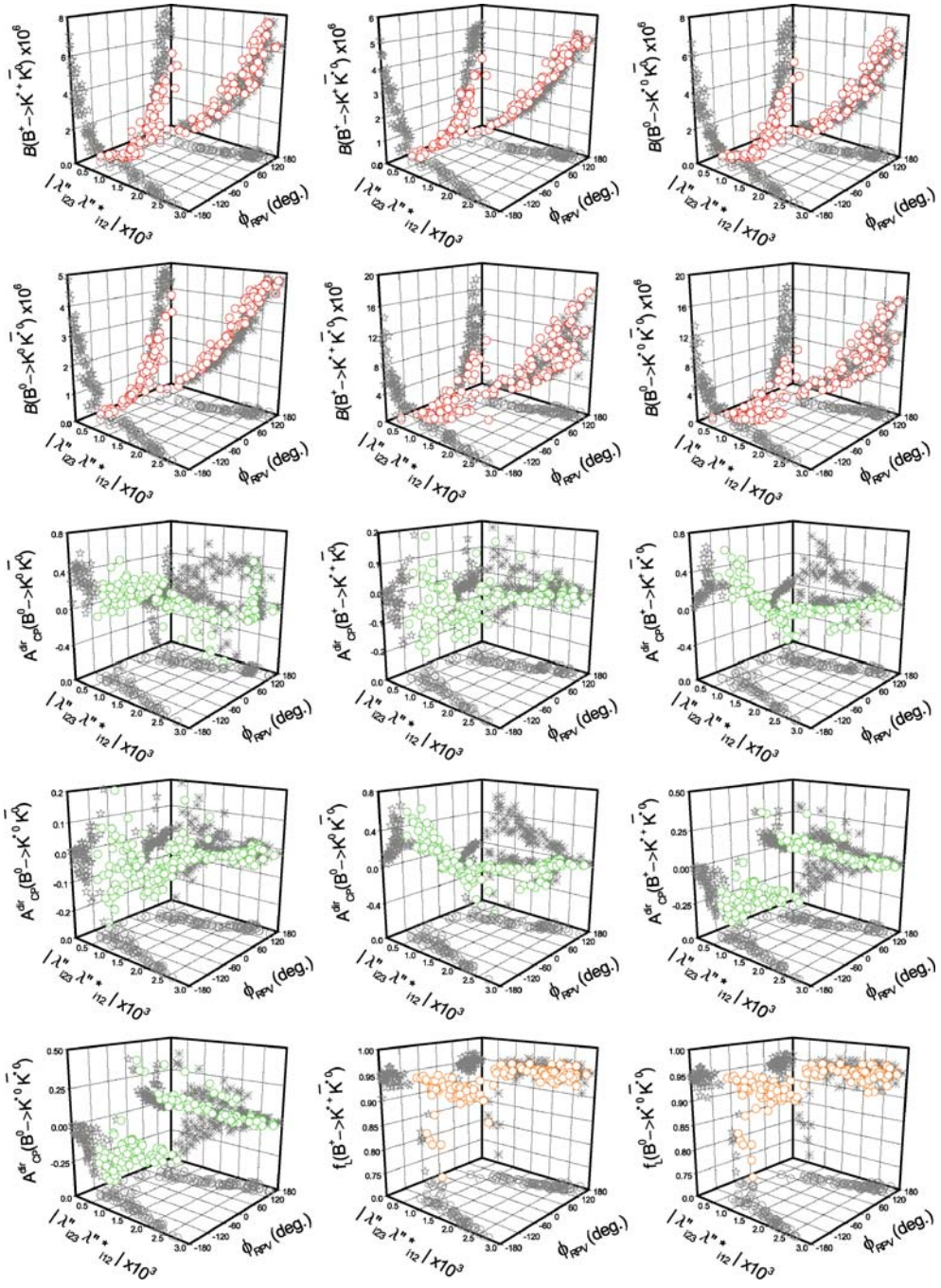

Fig. 6. The effects of RPV coupling $\lambda''_{i23}\lambda''^{*}_{i12}$ in $B \to K^{(*)}\bar{K}^{(*)}$ decays

strained RPV coupling spaces. Then the allowed ranges for $\mathcal{B}$, $\mathcal{A}_{CP}^{\rm dir}$ and $f_{\rm L}$ are obtained with five different RPV couplings, which satisfy all present experimental constraints shown in (29).

We obtain that the RPV effects could alter the predicted $\mathcal{B}$ and $\mathcal{A}_{CP}^{\rm dir}$ significantly from their SM values. For the decay modes, which have not been measured yet, their branching ratios can be changed one or two order(s) of magnitude compared with the SM expectations,

$$9.0\times10^{-9} < \mathcal{B}(B \to K^{+}\bar{K}^{*0}, K^{0}\bar{K}^{*0}) < 5.0\times10^{-6}\,,$$
$$5.0\times10^{-9} < \mathcal{B}(B \to K^{*+}\bar{K}^{0}, K^{*0}\bar{K}^{0}) < 8.0\times10^{-6}\,,$$
$$3.0\times10^{-8} < \mathcal{B}(B \to K^{*+}\bar{K}^{*0}, K^{*0}\bar{K}^{*0}) < 2.0\times10^{-5}\,, \quad (30)$$

especially, the upper limit of $\mathcal{B}(B \to K^{*+}\bar{K}^{*0}) < 2.0\times10^{-5}$ which we have obtained is smaller than the experimental upper limit $< 7.0\times10^{-5}$. For $\mathcal{A}_{CP}^{\rm dir}$, the RPV predictions on two decays $B \to K^{*+}\bar{K}^{*0}, K^{*0}\bar{K}^{*0}$ are

$$\mathcal{A}_{CP}^{\rm dir}(B \to K^{*+}\bar{K}^{*0}) \le 0.32\,,$$
$$\mathcal{A}_{CP}^{\rm dir}(B \to K^{*0}\bar{K}^{*0}) \le 0.38\,, \quad (31)$$

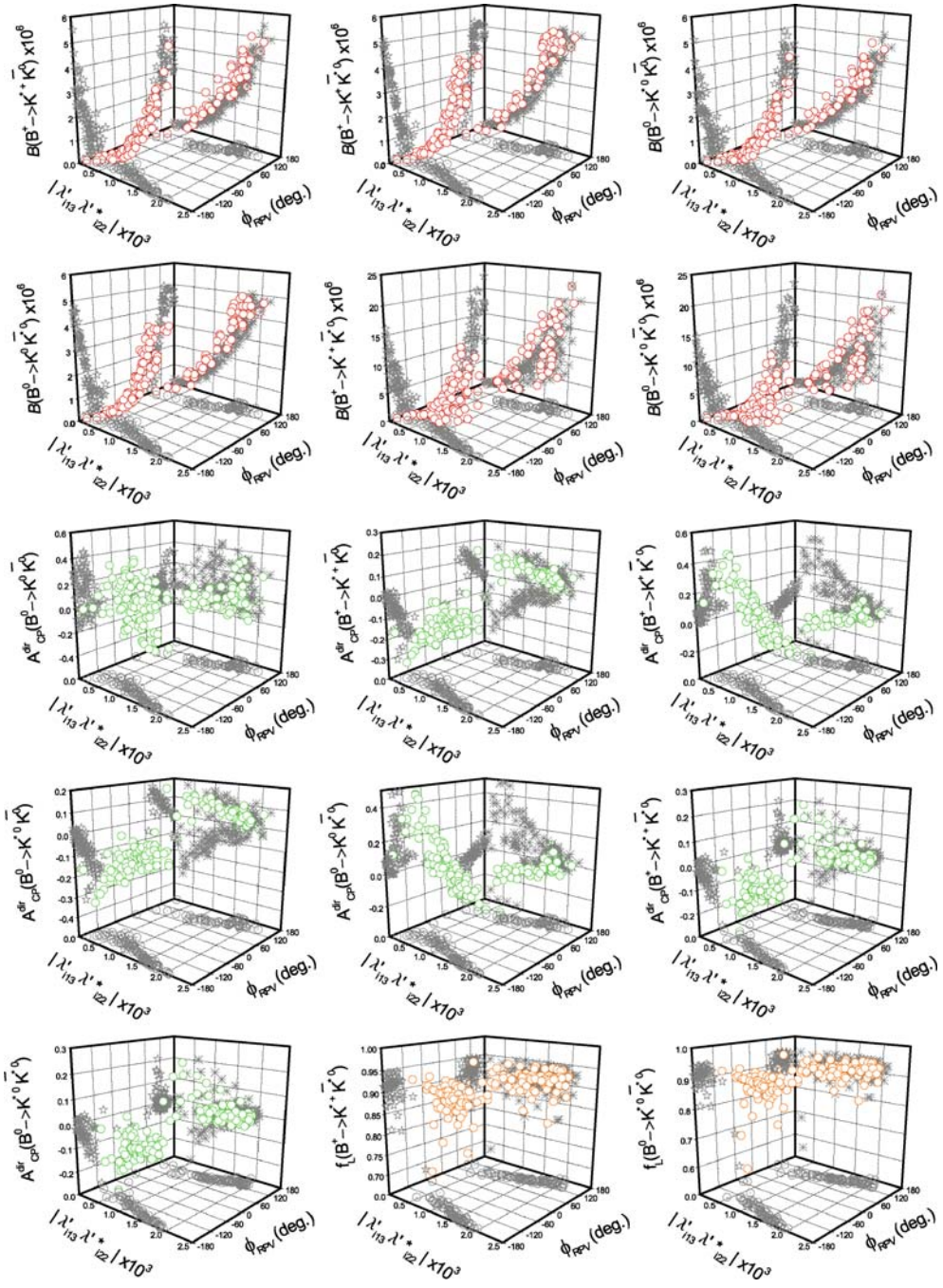

Fig. 7. The effects of RPV coupling $\lambda'_{i13}\lambda'^{*}_{i22}$ in $B \to K^{(*)}\bar{K}^{(*)}$ decays

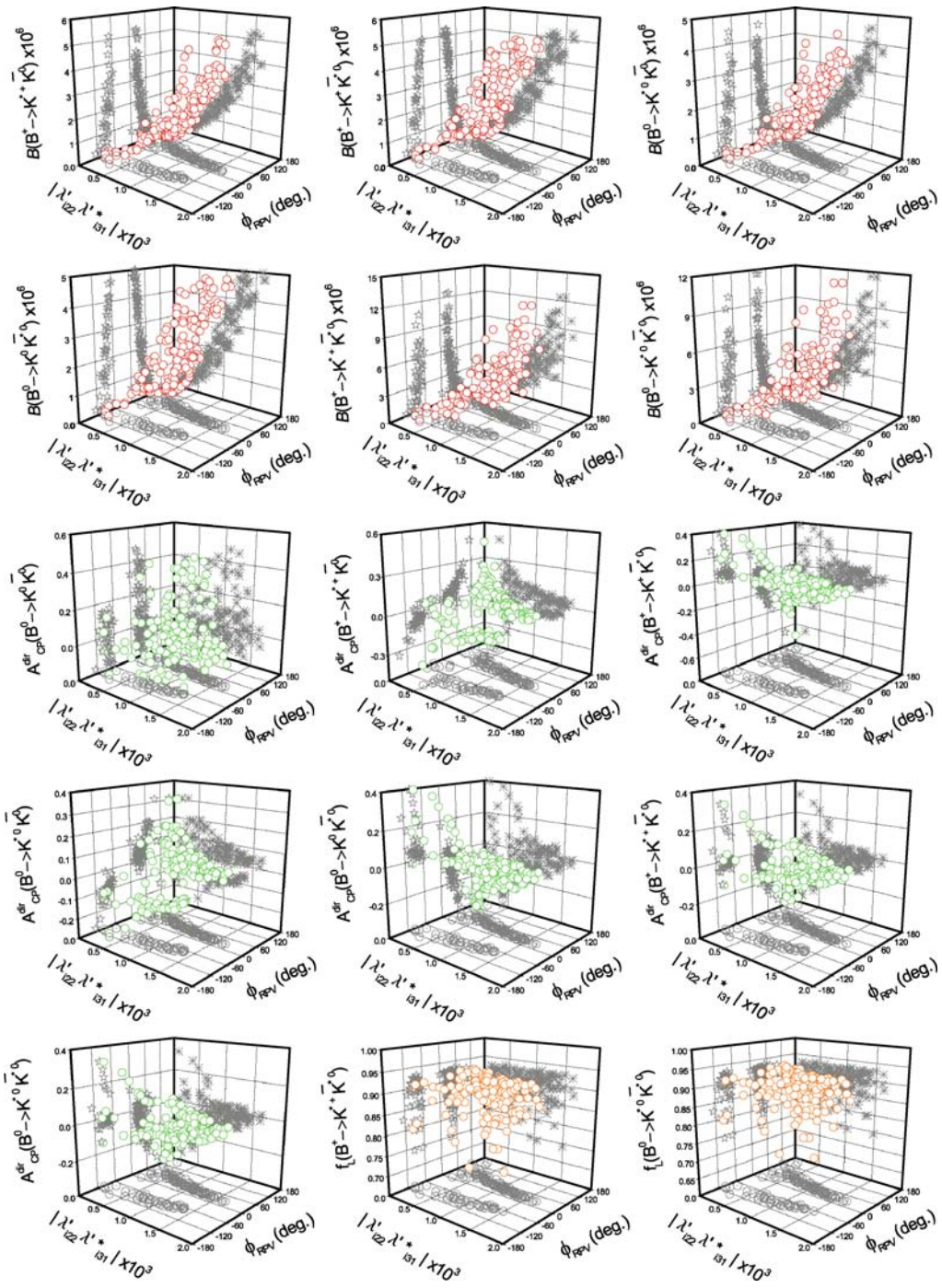

Fig. 8. The effects of RPV coupling $\lambda'_{i22}\lambda'^{*}_{i31}$ in $B \to K^{(*)}\bar{K}^{(*)}$ decays

and there are quite loose constraints on the direct CP asymmetries of the other five decays $B \to K^0\bar{K}^0, K^{*+}\bar{K}^0, K^+\bar{K}^{*0}, K^{*0}\bar{K}^0, K^0\bar{K}^{*0}$. But the RPV effects on the $f_{\rm L}(B \to K^{*+}\bar{K}^{*0}, K^{*0}\bar{K}^{*0})$ are found to be very small; $f_{\rm L}(B \to K^{*+}\bar{K}^{*0}, K^{*0}\bar{K}^{*0})$ are found to lie between 0.7 and 1, and these intervals are mainly due to the parameter uncertainties, not the RPV effects. So we might come to the conclusion that the RPV SUSY predictions show that the decays $B \to K^{*+}\bar{K}^{*0}, K^{*0}\bar{K}^{*0}$ are dominated by the longitudinal polarization, and there are not abnormal large transverse polarizations in the $B_{u,d} \to K^*\bar{K}^*$ decays. The detailed numerical ranges which we obtained by different RPV couplings are summarized in Table 3.

In Figs. 6–10, we present correlations between the physical observable $\mathcal{B}$, $\mathcal{A}_{CP}^{\rm dir}$, $f_{\rm L}$ and the parameter spaces of different RPV couplings by the three-dimensional scatter plots. More information is displayed in Figs. 6-10, and we can see the trends in the changes of the physical observable quantities with the modulus and weak phase ϕ_{R_p} of the RPV couplings. We take the first plot in Fig. 6 as an example; this plot shows that $\mathcal{B}(B \to K^{*+}\bar{K}^0)$ changes

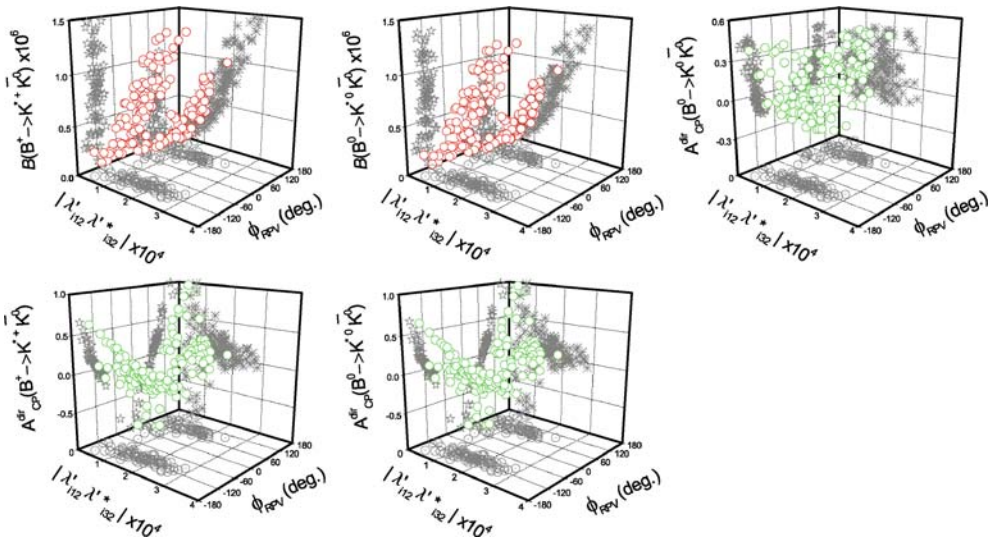

Fig. 9. The effects of RPV coupling $\lambda'_{i12}\lambda'^{*}_{i32}$ in $B \to K^{(*)}\bar{K}^{(*)}$ decays

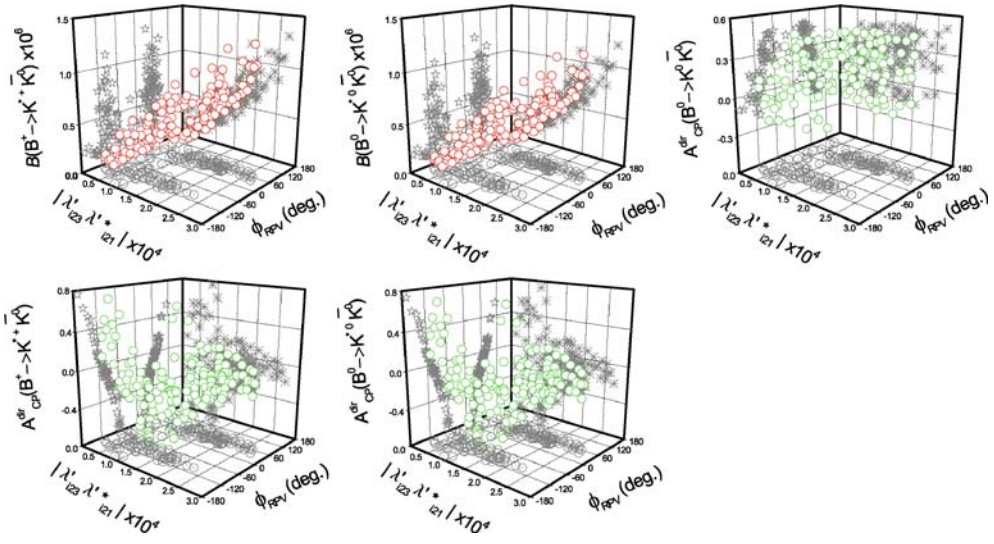

Fig. 10. The effects of RPV coupling $\lambda'_{i23}\lambda'^{*}_{i21}$ in $B \to K^{(*)}\bar{K}^{(*)}$ decays

with RPV coupling $\lambda''_{i23}\lambda''^{*}_{i12}$. We also give projections on three vertical planes; the $|\lambda''_{i23}\lambda''^{*}_{i12}|$–$\phi_{R\!\!/_p}$ plane displays the allowed regions of $\lambda''_{i23}\lambda''^{*}_{i12}$ which satisfy the experimental data in (29) (the same as the first plot in Fig. 5). It is shown that $\mathcal{B}(B \to K^{*+}\bar{K}^0)$ is increasing with $|\lambda''_{i23}\lambda''^{*}_{i12}|$ on the $\mathcal{B}(B \to K^{*+}\bar{K}^0)$–$|\lambda''_{i23}\lambda''^{*}_{i12}|$ plane. From the $\mathcal{B}(B \to K^{*+}\bar{K}^0)$–$\phi_{R\!\!/_p}$ plane, we can see that $\mathcal{B}(B \to K^{*+}\bar{K}^0)$ is increasing with $|\phi_{R\!\!/_p}|$. Further refined measurements of $\mathcal{B}(B \to K^{*+}\bar{K}^0)$ can further restrict the constrained space of $\lambda''_{i23}\lambda''^{*}_{i12}$, whereas with a narrower space of $\lambda''_{i23}\lambda''^{*}_{i12}$ a more accurate $\mathcal{B}(B \to K^{*+}\bar{K}^0)$ can be predicted.

The following salient features in Figs. 6-10 are a summary.

– Figure 6 displays the effects of the RPV coupling $\lambda''_{i23}\lambda''^{*}_{i12}$ on $\mathcal{B}$, $\mathcal{A}^{\rm dir}_{CP}$ and $f_{\rm L}$ in $B \to K^{(*)}\bar{K}^{(*)}$. The constrained $|\lambda''_{i23}\lambda''^{*}_{i12}|$–$\phi_{R\!\!/_p}$ plane shows the allowed range of $\lambda''_{i23}\lambda''^{*}_{i12}$ as in the first plot of Fig. 5. The six decays $\mathcal{B}(B \to K^{*+}\bar{K}^0, K^+\bar{K}^{*0}, K^{*0}\bar{K}^0, K^0\bar{K}^{*0}, K^{*+}\bar{K}^{*0}, K^{*0}\bar{K}^{*0})$ have the similar change with $|\lambda''_{i23}\lambda''^{*}_{i12}|$ and $|\phi_{R\!\!/_p}|$, and they are increasing with $|\lambda''_{i23}\lambda''^{*}_{i12}|$ and $|\phi_{R\!\!/_p}|$. The $|\mathcal{A}^{\rm dir}_{CP}(B \to K^0\bar{K}^0)|$ are increasing with $|\phi_{R\!\!/_p}|$, but $|\lambda''_{i23}\lambda''^{*}_{i12}|$ has a small effect on $\mathcal{A}^{\rm dir}_{CP}(B \to K^0\bar{K}^0)$. The two quantities $|\mathcal{A}^{\rm dir}_{CP}(B \to K^+\bar{K}^{*0}, K^0\bar{K}^{*0})|$ tend to zero with increasing $|\lambda''_{i23}\lambda''^{*}_{i12}|$ and $|\phi_{R\!\!/_p}|$. The other four, $|\mathcal{A}^{\rm dir}_{CP}(B \to K^{*+}\bar{K}^0, K^{*0}\bar{K}^0, K^{*+}\bar{K}^{*0}, K^{*0}\bar{K}^{*0})|$, tend to zero with increasing $|\phi_{R\!\!/_p}|$, and they could have smaller ranges with $|\lambda''_{i23}\lambda''^{*}_{i12}|$. The RPV effects on the $f_{\rm L}(B \to K^{*+}\bar{K}^{*0}, K^{*0}\bar{K}^{*0})$ are very small, and the $f_{\rm L}(B \to K^{*+}\bar{K}^{*0}, K^{*0}\bar{K}^{*0})$ are found to lie between 0.72 and 0.97.

– The effects of $\lambda'_{i13}\lambda'^{*}_{i22}$ on $\mathcal{B}$, $\mathcal{A}^{\rm dir}_{CP}$ and $f_{\rm L}$ are exhibited in Fig. 7. The constrained $|\lambda'_{i13}\lambda'^{*}_{i22}|$–$\phi_{R\!\!/_p}$ plane is the same as the second plot in Fig. 5. The effects of $\lambda'_{i13}\lambda'^{*}_{i22}$ on $\mathcal{B}$, $\mathcal{A}^{\rm dir}_{CP}$ and $f_{\rm L}$ are similar to $\lambda''_{i23}\lambda''^{*}_{i12}$ shown in Fig. 6.

– In Fig. 8, we plot $\mathcal{B}$, $\mathcal{A}^{\rm dir}_{CP}$ and $f_{\rm L}$ as functions of $\lambda'_{i22}\lambda'^{*}_{i31}$. The constrained $|\lambda'_{i22}\lambda'^{*}_{i31}|$–$\phi_{R\!\!/_p}$ plane is the

same as the third plot of Fig. 5. The six branching ratios are increasing with $|\lambda'_{i22}\lambda'^{*}_{i31}|$ and decreasing with $|\phi_{B_p}|$. $|\mathcal{A}_{CP}^{\rm dir}(B \to K^0\bar{K}^0)|$ is unaffected by $|\lambda'_{i22}\lambda'^{*}_{i31}|$, but the other six direct CP asymmetries could have smaller ranges with $|\lambda'_{i22}\lambda'^{*}_{i31}|$. $|\mathcal{A}_{CP}^{\rm dir}(K^{*+}\bar{K}^0, K^{*0}\bar{K}^0)|$ tends to zero with decreasing $|\phi_{B_p}|$; however, ϕ_{B_p} has a small effect on $\mathcal{A}_{CP}^{\rm dir}(B \to K^0\bar{K}^0, K^+\bar{K}^{*0}, K^0\bar{K}^{*0}, K^{*+}\bar{K}^{*0}, K^{*0}\bar{K}^{*0})$. The $\lambda'_{i22}\lambda'^{*}_{i31}$ effects on the $f_{\rm L}(B \to K^{*+}\bar{K}^{*0}, K^{*0}\bar{K}^{*0})$ are small.

– The RPV coupling $\lambda'_{i12}\lambda'^{*}_{i32}$ contributes to the decays $B \to K^+\bar{K}^0, K^0\bar{K}^0, K^{*+}\bar{K}^0, K^{*0}\bar{K}^0$, and the effects are shown in Fig. 9. The constrained $|\lambda'_{i12}\lambda'^{*}_{i32}|$–$\phi_{B_p}$ plane is the same as the fourth plot in Fig. 5. We can see that $\mathcal{B}(B \to K^{*+}\bar{K}^0, K^{*0}\bar{K}^0)$ are rising with $|\lambda'_{i12}\lambda'^{*}_{i32}|$ and unaffected by ϕ_{B_p}. $\mathcal{A}_{CP}^{\rm dir}(B \to K^0\bar{K}^0)$ is steady against $|\lambda'_{i12}\lambda'^{*}_{i32}|$, and $|\mathcal{A}_{CP}^{\rm dir}(B \to K^{*+}\bar{K}^0, K^{*0}\bar{K}^0)|$ could have smaller ranges with $|\lambda'_{i12}\lambda'^{*}_{i32}|$. $\mathcal{A}_{CP}^{\rm dir}(B \to K^0\bar{K}^0, K^{*+}\bar{K}^0, K^{*0}\bar{K}^0)$ are becoming large with increasing of $|\phi_{B_p}|$.
– $\lambda'_{i23}\lambda'^{*}_{i21}$ also only contributes to the decays $B \to K^+\bar{K}^0, K^0\bar{K}^0, K^{*+}\bar{K}^0, K^{*0}\bar{K}^0$, and its effects are shown in Fig. 10. The constrained $|\lambda'_{i23}\lambda'^{*}_{i21}|$–$\phi_{B_p}$ plane is the same as the last plot in Fig. 5. $\mathcal{B}(B \to K^{*+}\bar{K}^0, K^{*0}\bar{K}^0)$ are increasing with $|\lambda'_{i23}\lambda'^{*}_{i21}|$ and unaffected by ϕ_{B_p}. $\mathcal{A}_{CP}^{\rm dir}(B \to K^0\bar{K}^0)$ is steady against $|\lambda'_{i23}\lambda'^{*}_{i21}|$, and $|\mathcal{A}_{CP}^{\rm dir}(B \to K^{*+}\bar{K}^0, K^{*0}\bar{K}^0)|$ could be varied in small ranges with $|\lambda'_{i23}\lambda'^{*}_{i21}|$. $\mathcal{A}_{CP}^{\rm dir}(B \to K^0\bar{K}^0)$ is decreasing with $|\phi_{B_p}|$, but the $\mathcal{A}_{CP}^{\rm dir}(B \to K^{*+}\bar{K}^0, K^{*0}\bar{K}^0)$ are increasing with $|\phi_{B_p}|$.

The predictions of $\mathcal{B}$ and $\mathcal{A}_{CP}^{\rm dir}$ are quite uncertain in the RPV SUSY, since we just have a few experimental measurements and many theoretical uncertainties. One must wait for the error bars to come down and more channels to be measured. With the operation of B factory experiments, large amounts of experimental data on hadronic B-meson decays are being collected, and measurements of previously known observables will become more precise. From the comparison of our predictions in Figs. 6–10 with the near future experiments, one will obtain more stringent bounds on the product combinations of the RPV couplings. On the other hand, the RPV SUSY predictions of other decays will become more precise by the more stringent bounds on the RPV couplings.

5 Conclusions

In conclusion, the pure penguin $B \to K^{(*)}\bar{K}^{(*)}$ decays are very important for understanding of the dynamics of nonleptonic two-body B decays and testing the SM. We have studied the $B \to K^{(*)}\bar{K}^{(*)}$ decays with the QCDF approach in the RPV SUSY model. We have obtained fairly constrained parameter spaces of the RPV couplings from the present experimental data of $B \to K^{(*)}\bar{K}^{(*)}$ decays, and some of these constraints are stronger than the existing ones. Furthermore, using the constrained parameter spaces, we have shown the RPV SUSY expectations for the other quantities in $B \to K^{(*)}\bar{K}^{(*)}$ decays which have not been measured yet. We have found that the RPV effects could significantly alter $\mathcal{B}$ and $\mathcal{A}_{CP}^{\rm dir}$ from their SM values, but the $f_{\rm L}(B \to K^{*+}\bar{K}^{*0}, K^{*0}\bar{K}^{*0})$ are not significantly affected by the RPV effects and the decays $B \to K^{*+}\bar{K}^{*0}, K^{*0}\bar{K}^{*0}$ are still dominated by the longitudinal polarization. We also have presented correlations between the physical observables $\mathcal{B}$, $\mathcal{A}_{CP}^{\rm dir}$, $f_{\rm L}$ and the constrained parameter spaces of the RPV couplings in Figs. 6–10, which could be tested in the near future.

Acknowledgements. The work is supported by National Science Foundation under contract No. 10305003, Henan Provincial Foundation for Prominent Young Scientists under contract No. 0312001700 and the NCET Program sponsored by Ministry of Education, China. Furthermore, this work is supported by National Natural Science Foundation of China under projects 10440420018, 10475031 and 10135030, and by MOE of China under projects NCET-04-0744, SRFDP-20040511005, CFKSTIP-704035.

Appendix A: Correction functions for $B \to M_1M_2$ decay at $\alpha_{\rm s}$ order

In this appendix, we present the explicit form for the correction functions appearing in the parameters a_i^p and b_i^p. It is noted that in $B \to PV$ decays, $\Phi_M(u) \to \Phi_\parallel^V(u)$ if M is a vector meson.

A.1 The correction functions in $B \to PP, PV$ decays

• The one-loop vertex correction function is

$$V_{M_2} = 12\ln\frac{m_b}{\mu} - 18 + 3\int_0^1 {\rm d}u \left(\frac{1-2u}{1-u}\ln u - {\rm i}\pi\right)\Phi_{M_2}(u)\,. \tag{A.1}$$

• The hard spectator interactions are given by

$$H_{M_1M_2} = \frac{4\pi^2}{N_C}\frac{f_B f_{M_1}}{m_B^2 F_0^{B\to M_1}(m_{M_2}^2)}\int_0^1 \frac{{\rm d}\xi}{\xi}\Phi_1^B(\xi) \times \int_0^1 \frac{{\rm d}u}{\bar{u}}\Phi_{M_2}(u) \times \int_0^1 \frac{{\rm d}v}{\bar{v}}\left[\Phi_{M_1}(v) + \frac{2\mu_{M_1}}{M_B}\Phi_p^{M_1}(v)\right], \tag{A.2}$$

if M_2 is a pseudoscalar meson, and

$$H_{M_1M_2} = \frac{4\pi^2}{N_C}\frac{f_B f_{M_1}}{m_B^2 A_0^{B\to M_1}(m_{M_2}^2)}\int_0^1 \frac{{\rm d}\xi}{\xi}\Phi_1^B(\xi) \times \int_0^1 \frac{{\rm d}u}{\bar{u}}\Phi_{M_2}(u)\int_0^1 \frac{{\rm d}v}{\bar{v}}\Phi_{M_1}(v)\,, \tag{A.3}$$

if M_2 is a vector meson.

Considering the off-shellness of the gluon in the hard-scattering kernel, it is natural to associate a scale $\mu_h \sim \sqrt{\Lambda_{\rm QCD} m_b}$, rather than $\mu \sim m_b$. For the logarithmically

divergent integral, we will parameterize it as in [17]: $X_H = \int_0^1 \mathrm{d}u/u = -\ln(\Lambda_{\rm QCD}/m_b) + \varrho_H \mathrm{e}^{\mathrm{i}\phi_H} \quad m_b/\Lambda_{\rm QCD}$ with (ϱ_H, ϕ_H) related to the contributions from hard spectator scattering. In the numerical analysis, we take $\Lambda_{\rm QCD} = 0.5\,\mathrm{GeV}$, $(\varrho_h, \phi_H) = (0,0)$ as our default values. We have the same as in $B \to VV$ decay.

• The penguin contributions at twist-2 are described by the functions

$$\begin{aligned} P^p_{M_2,2} &= C_1 G_{M_2}(s_p) + C_3\Big[G_{M_2}(0) + G_{M_2}(1)\Big] \\ &\quad + (C_4 + C_6) \\ &\quad \times \left[(n_{\rm f}-2)G_{M_2}(0) + G_{M_2}(s_c) + G_{M_2}(1) - \frac{2n_{\rm f}}{3}\right] \\ &\quad - C^{\rm eff}_{8g}\int_0^1 \mathrm{d}u\,\frac{2\Phi_{M_2}(u)}{1-u}\,, \\ P^{p,\rm EW}_{M_2,2} &= (C_1 + N_C C_2)G_{M_2}(s_p) - C^{\rm eff}_{7\gamma}\int_0^1 \mathrm{d}u\,\frac{3\Phi_{M_2}(u)}{1-u}\,, \end{aligned} \tag{A.4}$$

where $n_f = 5$ is the number of quark flavors, and $s_u = 0, s_c = (m_c/m_b)^2$ are the mass ratios involved in the evaluation of the penguin diagrams. The function $G_{M_2}(s)$ is defined as

$$\begin{aligned} G_{M_2}(s) &= \frac{2}{3} + \frac{4}{3}\ln\frac{m_b}{\mu} \\ &\quad + 4\int_0^1 \mathrm{d}u \int_0^1 \mathrm{d}x\, x\bar{x}\ln(s - x\bar{x}\bar{u} - \mathrm{i}\epsilon)\Phi_{M_2}(u)\,. \end{aligned} \tag{A.5}$$

• The twist-3 terms from the penguin diagrams are given by

$$\begin{aligned} P^p_{M_2,3} &= C_1\widehat{G}_{M_2}(s_p) + C_3\left[\widehat{G}_{M_2}(0) + \widehat{G}_{M_2}(1)\right] \\ &\quad + (C_4 + C_6)\Big[(n_{\rm f}-2)\widehat{G}_{M_2}(0) \\ &\quad + \widehat{G}_{M_2}(s_c) + \widehat{G}_{M_2}(1) - \frac{2n_{\rm f}}{3}\Big] - 2C^{\rm eff}_{8g}, \\ P^{p,\rm EW}_{M_2,3} &= (C_1 + N_C C_2)\widehat{G}_{M_2}(s_p) - 3C^{\rm eff}_{7\gamma}\,, \end{aligned} \tag{A.6}$$

with

$$\begin{aligned} \widehat{G}_{M_2}(s) &= \frac{2}{3} + \frac{4}{3}\ln\frac{m_b}{\mu} \\ &\quad + 4\int_0^1 \mathrm{d}u \int_0^1 \mathrm{d}x\, x\bar{x}\ln(s - x\bar{x}\bar{u} - \mathrm{i}\epsilon)\Phi^{M_2}_p(u)\,, \end{aligned} \tag{A.7}$$

if M_2 is a pseudoscalar meson, and we omit the twist-3 terms from the penguin diagrams when M_2 is a vector meson.

• The weak annihilation contributions are given by

$$\begin{aligned} A^i_1(M_1,M_2) &\approx A^i_2(M_1,M_2) \\ &\approx \pi\alpha_{\rm s}\left[18\left(X_A - 4 + \frac{\pi^2}{3}\right) + 2r^{M_1}_\chi r^{M_2}_\chi X_A^2\right], \\ A^i_3(M_1,M_2) &\approx 6\pi\alpha_{\rm s}\left(r^{M_1}_\chi - r^{M_2}_\chi\right)\left(X_A^2 - 2X_A + \frac{\pi^2}{3}\right), \\ A^f_3(M_1,M_2) &\approx 6\pi\alpha_{\rm s}\left(r^{M_1}_\chi + r^{M_2}_\chi\right)\left(2X_A^2 - X_A\right), \\ A^f_1(M_1,M_2) &= 0, \quad A^f_2(M_1,M_2) = 0\,, \end{aligned} \tag{A.8}$$

when both final state mesons are pseudoscalar, whereas

$$\begin{aligned} A^i_1(M_1,M_2) &\approx -A^i_2(M_1,M_2) \approx 18\pi\alpha_{\rm s}\left(X_A - 4 + \frac{\pi^2}{3}\right), \\ A^i_3(M_1,M_2) &\approx 6\pi\alpha_{\rm s} r^{M_1}_\chi\left(X_A^2 - 2X_A + \frac{\pi^2}{3}\right), \\ A^f_3(M_1,M_2) &\approx -6\pi\alpha_{\rm s} r^{M_1}_\chi\left(2X_A^2 - X_A\right), \\ A^f_1(M_1,M_2) &= 0, \quad A^f_2(M_1,M_2) = 0\,, \end{aligned} \tag{A.9}$$

when M_1 is a vector meson and M_2 is a pseudoscalar. For the opposite case of a pseudoscalar M_1 and a vector M_2, one exchanges $r^{M_1}_\chi \leftrightarrow r^{M_2}_\chi$ in the previous equations and changes the sign of A^f_3.

Here the superscripts i and f refer to gluon emission from the initial and final state quarks, respectively. The subscript k of $A^{i,f}_k$ refers to one of the three possible Dirac structures $\Gamma_1 \otimes \Gamma_2$, namely $k = 1$ for $(V-A)\otimes(V-A)$, $k = 2$ for $(V-A)\otimes(V+A)$, and $k = 3$ for $(-2)(S-P)\otimes(S+P)$. $X_A = \int_0^1 \mathrm{d}u/u$ is a logarithmically divergent integral, and will be phenomenologically parameterized in the calculation as X_H. As for the hard spectator terms, we will evaluate the various quantities in (A.8) and (A.9) at the scale $\mu_h = \sqrt{\Lambda_{\rm QCD} m_b}$.

A.2 $B \to VV$ decays

In the rest frame of the B system, since the B-meson has spin zero, two vectors have the same helicity; therefore, three polarization states are possible, one longitudinal (L) and two transverse, corresponding to helicities $\lambda = 0$ and $\lambda = \pm$ (here $\lambda_1 = \lambda_2 = \lambda$). We assume the M_1- (M_2-) meson to be flying in the minus (plus) z-direction carrying the momentum p_1 (p_2), Using the sign convention $\epsilon^{0123} = -1$, we have

$$A_{M_1M_2} = \begin{cases} \frac{\mathrm{i}f_{M_2}}{2m_{M_1}}\Big[\left(m_B^2 - m_{M_1}^2 - m_{M_2}^2\right)(m_B + m_{M_1}) \\ \quad \times A_1^{B\to M_1}\left(m_{M_2}^2\right) - \frac{4m_B^2 p_{\rm c}^2}{m_B + m_{M_1}} \\ \quad \times A_2^{B\to M_1}\left(m_{M_2}^2\right)\Big] \equiv h_0\,, \\ \mathrm{i}f_{V_2} m_{M_2}[(m_B + m_{M_1})\,A_1^{B\to M_1}\left(m_{M_2}^2\right) \\ \quad \mp \frac{2m_B p_{\rm c}}{m_B + m_{M_1}} V^{B\to M_1}\left(m_{M_2}^2\right)] \equiv h_\pm\,, \end{cases} \tag{A.10}$$

where h_0 for $\lambda = 0$ and $h_\pm$ for $\lambda = \pm$.

• $V^{\lambda}_{M_2}(\pm 1)$ contain the contributions from the vertex corrections and are given by

$$V^{0}_{M_2}(a) = 12\ln\frac{m_b}{\mu} - 18 + \int_0^1 \mathrm{d}u \Phi^{M_2}_{\parallel}(u)\left(3\frac{1-2u}{1-u}\ln u - 3\mathrm{i}\pi\right), \tag{A.11}$$

$$V^{\pm}_{M_2}(a) = 12\ln\frac{m_b}{\mu} - 18 + \int_0^1 \mathrm{d}u \left(\mathrm{g}^{(v)M_2}_{\perp}(u) \pm \frac{a\mathrm{g}^{\prime(a)M_2}_{\perp}(u)}{4}\right) \times \left(3\frac{1-2u}{1-u}\ln u - 3\mathrm{i}\pi\right).$$

• For the hard spectator-scattering contributions, explicit calculations for $H^{\lambda}_{M_1M_2}(a)$ yield

$$H^{0}_{M_1M_2}(a) = \frac{4\pi^2}{N_C}\frac{\mathrm{i}f_B f_{V_1} f_{V_2}}{h_0}\int_0^1 \mathrm{d}\xi \frac{\Phi^B_1(\xi)}{\xi}\int_0^1 \mathrm{d}v \frac{\Phi^{M_1}_{\parallel}(v)}{\bar{v}} \times \int_0^1 \mathrm{d}u \frac{\Phi^{M_2}_{\parallel}(u)}{u},$$

$$H^{\pm}_{M_1M_2}(a) = -\frac{4\pi^2}{N_C}\frac{2\mathrm{i}f_B f^{\perp}_{M_1} f_{M_2} m_{M_2}}{m_B h_{\pm}}(1\mp 1) \times \int_0^1 \mathrm{d}\xi \frac{\Phi^B_1(\xi)}{\xi}\int_0^1 \mathrm{d}v \frac{\Phi^{M_1}_{\perp}(v)}{\bar{v}^2} \times \int_0^1 \mathrm{d}u \left(\mathrm{g}^{(v)M_2}_{\perp}(u) - \frac{a\mathrm{g}^{\prime(a)M_2}_{\perp}(u)}{4}\right) + \frac{4\pi^2}{N_C}\frac{2\mathrm{i}f_B f_{M_1} f_{M_2} m_{M_1} m_{M_2}}{m_B^2 h_{\pm}}\int_0^1 \mathrm{d}\xi \frac{\Phi^B_1(\xi)}{\xi} \times \int_0^1 \mathrm{d}v\mathrm{d}u \left(\mathrm{g}^{(v)M_1}_{\perp}(v) \pm \frac{\mathrm{g}^{\prime(a)M_1}_{\perp}(v)}{4}\right) \times \left(\mathrm{g}^{(v)M_2}_{\perp}(u) \pm \frac{a\mathrm{g}^{\prime(a)M_2}_{\perp}(u)}{4}\right)\frac{u+\bar{v}}{u\bar{v}^2}, \tag{A.12}$$

with $\bar{v} = 1 - v$; when the asymptotical forms for the vector meson LCDAs are adopted, there will be infrared divergences in $H^{\pm}_{M_1M_2}$. As in [16, 28], we introduce a cutoff of order $\Lambda_{\mathrm{QCD}}/m_b$ and take $\Lambda_{\mathrm{QCD}} = 0.5\,\mathrm{GeV}$ as our default value.

• The contributions of the QCD penguin-type diagrams can be described by the functions

$$P^{\lambda,p}_{M_2,2} = C_1 G^{\lambda}_{M_2}(s_p) + C_3\left[G^{\lambda}_{M_2}(s_q) + G^{\lambda}_{M_2}(s_b)\right] + (C_4 + C_6)\sum_{q'=u}^{b}\left[G^{\lambda}_{M_2}(s_{q'}) - \frac{2}{3}\right] + \frac{3}{2}C_9\left[e_q G^{\lambda}_{M_2}(s_q) + e_b G^{\lambda}_{M_2}(s_b)\right] + \frac{3}{2}(C_8 + C_{10})\sum_{q'=u}^{b} e_{q'}\left[G^{\lambda}_{M_2}(s_{q'}) - \frac{2}{3}\right] + C^{\mathrm{eff}}_{8g} G^{\lambda}_{g},$$

$$P^{\lambda,p,\mathrm{EW}}_{M_2,2} = (C_1 + N_C C_2)\left[\frac{2}{3} + \frac{4}{3}\ln\frac{m_b}{\mu} - G^{\lambda}_{M_2}(s_p)\right] + \frac{3}{2}C^{\mathrm{eff}}_{7\gamma} G^{\lambda}_{g}, \tag{A.13}$$

$$G^{0}_{M_2}(s) = \frac{2}{3} + \frac{4}{3}\ln\frac{m_b}{\mu} + 4\int_0^1 \mathrm{d}u\, \Phi^{M_2}_{\parallel}(u)\mathrm{g}(u,s),$$

$$G^{\pm}_{M_2}(s) = \frac{2}{3} + \frac{2}{3}\ln\frac{m_b}{\mu} + 2\int_0^1 \mathrm{d}u\, (\mathrm{g}^{(v)M_2}_{\perp}(u) \pm \frac{\mathrm{g}^{\prime(a)M_2}_{\perp}(u)}{4})\mathrm{g}(u,s), \tag{A.14}$$

with the function $\mathrm{g}(u,s)$ defined as

$$\mathrm{g}(u,s) = \int_0^1 \mathrm{d}x\, x\bar{x}\ln(s - x\bar{x}\bar{u} - \mathrm{i}\epsilon). \tag{A.15}$$

We omit the twist-3 terms from the penguin diagrams for $B \to VV$ decays.

• We have also taken into account the contributions of the dipole operator O_{8g}, which are described by the functions

$$G^{0}_{g} = -\int_0^1 \mathrm{d}u\, \frac{2\Phi^{M_2}_{\parallel}(u)}{1-u},$$

$$G^{\pm}_{g} = \int_0^1 \frac{\mathrm{d}u}{\bar{u}}\left[-\bar{u}\mathrm{g}^{(v)M_2}_{\perp}(u) \mp \frac{\bar{u}\mathrm{g}^{\prime(a)M_2}_{\perp}(u)}{4} + \int_0^u \mathrm{d}v\left(\Phi^{M_2}_{\parallel}(v) - \mathrm{g}^{(v)M_2}_{\perp}(v)\right) + \frac{\mathrm{g}^{(a)M_2}_{\perp}(u)}{4}\right], \tag{A.16}$$

here we consider the higher-twist effects $k^{\mu} = uEn^{\mu}_{-} + k^{\mu}_{\perp} + \frac{k^2_{\perp}}{4uE}n^{\mu}_{+}$ in the projector of the vector meson. The $G^{\pm}_{g} = 0$ in (A.16) [28, 30], if considering the Wandzura–Wilczek-type relations [29].

We have not onsidered the annihilation contributions in $B \to VV$ decays.

A.3 The contributions of new operators in RPV SUSY

Compared with the operators in the $\mathcal{H}^{\mathrm{SM}}_{\mathrm{eff}}$, there are new operators $(\bar{q}_2 q_3)_{V\pm A}(\bar{b}q_1)_{V+A}$ in the $\mathcal{H}^{\not{R}p}_{\mathrm{eff}}$.

• For $B \to PP, PV$ decays, since

$$\begin{aligned}
\langle P|\,\bar{q}_1\gamma_\mu(1-\gamma_5)q_2|\,0\rangle &= -\langle P|\,\bar{q}_1\gamma_\mu(1+\gamma_5)q_2|\,0\rangle \\
&= -\langle P|\,\bar{q}_1\gamma_\mu\gamma_5 q_2|\,0\rangle, \\
\langle P|\,\bar{q}\gamma_\mu(1-\gamma_5)b\mid B\rangle &= \langle P|\,\bar{q}\gamma_\mu(1+\gamma_5)b\mid B\rangle \\
&= \langle P|\,\bar{q}\gamma_\mu b\mid B\rangle, \\
\langle V|\,\bar{q}_1\gamma_\mu(1-\gamma_5)q_2|\,0\rangle &= \langle V|\,\bar{q}_1\gamma_\mu(1+\gamma_5)q_2|\,0\rangle \\
&= \langle V|\,\bar{q}_1\gamma_\mu q_2|\,0\rangle, \\
\langle V|\,\bar{q}\gamma_\mu(1-\gamma_5)b\mid B\rangle &= -\langle V|\,\bar{q}\gamma_\mu(1+\gamma_5)b\mid B\rangle \\
&= -\langle V|\,\bar{q}\gamma_\mu\gamma_5 b\mid B\rangle,
\end{aligned} \tag{A.17}$$

the RPV contribution to the decay amplitude will modify the SM amplitude by an overall relation.

• For $B \to VV$, we will use the prime on the quantities standing for the $(\bar{q}_2 q_3)_{V\pm A}(\bar{b}q_1)_{V+A}$ current contribution. In the NF approach, the factorizable amplitude can be expressed as

$$A'_{M_1M_2} = \langle M_2|(\bar{q}_2\gamma_\mu(1-a\gamma_5)q_3)|0\rangle \times \langle M_1|(\bar{b}\gamma^\mu(1+\gamma_5)q_1)|B\rangle\,. \quad \text{(A.18)}$$

Taking the M_1- (M_2-) meson flying in the minus (plus) z-direction and using the sign convention $\epsilon^{0123} = -1$, we have

$$A'_{M_1M_2} = \begin{cases} \frac{-\mathrm{i}f_{M_2}}{2m_{M_1}}\Big[\left(m_B^2 - m_{M_1}^2 - m_{M_2}^2\right)(m_B+m_{M_1}) \\ \quad \times A_1^{B\to M_1}\left(m_{M_2}^2\right) - \frac{2m_B^2 p_c^2}{m_B+m_{M_1}} \\ \quad \times A_2^{B\to M_1}\left(m_{M_2}^2\right)\Big] \equiv h'_0\,, \\ -\mathrm{i}f_{M_2}m_{M_2}\Big[(m_B+m_{M_1})\,A_1^{B\to M_1}\left(m_{M_2}^2\right) \\ \quad \pm\frac{2m_B p_c}{m_B+m_{M_1}}V^{B\to M_1}\left(m_{M_2}^2\right)\Big] \equiv h'_\pm\,. \end{cases} \quad \text{(A.19)}$$

The vertex corrections $V'^{\lambda}_{M_2}(a)$ and the hard spectator-scattering corrections $H'^{\lambda}_{M_1M_2}(a)$ as follows:

$$\begin{aligned} V'^{0}_{M_2}(a) &= -12\ln\frac{m_b}{\mu} + 18 - 6(1+a) \\ &\quad - \int_0^1 \mathrm{d}u\Phi_\parallel^{M_2}(u)\left(3\frac{1-2u}{1-u}\ln u - 3\mathrm{i}\pi\right), \\ V'^{\pm}_{M_2}(a) &= -12\ln\frac{m_b}{\mu} + 18 - 6(1+a) \\ &\quad - \int_0^1 \mathrm{d}u\left(g_\perp^{(v)M_2}(u) \pm \frac{a g_\perp^{\prime(a)M_2}(u)}{4}\right) \\ &\quad \times\left(3\frac{1-2u}{1-u}\ln u - 3\mathrm{i}\pi\right), \\ H'^{0}_{M_1M_2}(a) &= \frac{4\pi^2}{N_C}\frac{\mathrm{i}f_B f_{M_1} f_{M_2}}{h'_0}\int_0^1 \mathrm{d}\xi\frac{\Phi_1^B(\xi)}{\xi} \\ &\quad \times\int_0^1 \mathrm{d}v\frac{\Phi_\parallel^{M_1}(v)}{\bar{v}}\int_0^1 \mathrm{d}u\frac{\Phi_\parallel^{M_2}(u)}{u}\,, \\ H'^{\pm}_{M_1M_2}(a) &= -\frac{4\pi^2}{N_C}\frac{2\mathrm{i}f_B f_{M_1}^\perp f_{M_2} m_{M_2}}{m_B h'_\pm}(1\pm1)\int_0^1 \mathrm{d}\xi\frac{\Phi_1^B(\xi)}{\xi} \\ &\quad \times\int_0^1 \mathrm{d}v\frac{\Phi_\perp^{M_1}(v)}{\bar{v}^2} \\ &\quad \times\int_0^1 \mathrm{d}u\left(g_\perp^{(v)M_2}(u) + \frac{a g_\perp^{\prime(a)M_2}(u)}{4}\right) \\ &\quad + \frac{4\pi^2}{N_C}\frac{2\mathrm{i}f_B f_{M_1} f_{M_2} m_{M_1} m_{M_2}}{m_B^2 h'_\pm}\int_0^1 \mathrm{d}\xi\frac{\Phi_1^B(\xi)}{\xi} \\ &\quad \times\int_0^1 \mathrm{d}v\mathrm{d}u\left(g_\perp^{(v)M_1}(v) \mp \frac{g_\perp^{\prime(a)M_1}(v)}{4}\right) \\ &\quad \times\left(g_\perp^{(v)M_2}(u) \pm \frac{a\, g_\perp^{\prime(a)M_2}(u)}{4}\right)\frac{u+\bar{v}}{u\bar{v}^2}\,. \end{aligned} \quad \text{(A.20)}$$

Appendix B: The amplitudes in the SM

We have

$$\begin{aligned} &\mathcal{A}_f^{\mathrm{SM}}(B^+\to K^+\bar{K}^0) \\ &= \frac{G_\mathrm{F}}{\sqrt{2}}\Big\{-V_{tb}^*V_{td}\Big[a_4 - \frac{1}{2}a_{10} + r_\chi^{K^0}\left(a_6 - \frac{1}{2}a_8\right)\Big]\Big\}A_{K^+\bar{K}^0}\,, \end{aligned} \quad \text{(B.1)}$$

$$\begin{aligned} &\mathcal{A}_a^{\mathrm{SM}}(B^+\to K^+\bar{K}^0) \\ &= \mathrm{i}\frac{G_\mathrm{F}}{\sqrt{2}}f_B f_K^2\Big\{V_{ub}^*V_{ud}b_2(K^+,\bar{K}^0) \\ &\quad - V_{tb}^*V_{td}\Big[b_3(K^+,\bar{K}^0) + b_3^{\mathrm{EW}}(K^+,\bar{K}^0)\Big]\Big\}, \end{aligned} \quad \text{(B.2)}$$

$$\begin{aligned} &\mathcal{A}_f^{\mathrm{SM}}(B^0\to K^0\bar{K}^0) \\ &= \frac{G_\mathrm{F}}{\sqrt{2}}\Big\{-V_{tb}^*V_{td}\Big[a_4 - \frac{1}{2}a_{10} + r_\chi^{K^0}\left(a_6 - \frac{1}{2}a_8\right)\Big]\Big\}A_{K^0\bar{K}^0}\,, \end{aligned} \quad \text{(B.3)}$$

$$\begin{aligned} &\mathcal{A}_a^{\mathrm{SM}}(B^0\to K^0\bar{K}^0) \\ &= \mathrm{i}\frac{G_\mathrm{F}}{\sqrt{2}}f_B f_K^2\Big\{-V_{tb}^*V_{td}\Big[b_3(\bar{K}^0,K^0) + b_4(\bar{K}^0,K^0) \\ &\quad + b_4(K^0,\bar{K}^0) - \frac{1}{2}b_3^{\mathrm{EW}}(\bar{K}^0,K^0) - \frac{1}{2}b_4^{\mathrm{EW}}(\bar{K}^0,K^0) \\ &\quad - \frac{1}{2}b_4^{\mathrm{EW}}(K^0,\bar{K}^0)\Big]\Big\}, \end{aligned} \quad \text{(B.4)}$$

$$\begin{aligned} &\mathcal{A}_f^{\mathrm{SM}}(B^+\to K^{*+}\bar{K}^0) \\ &= \frac{G_\mathrm{F}}{\sqrt{2}}\Big\{-V_{tb}^*V_{td}\Big[a_4 - \frac{1}{2}a_{10} - r_\chi^{K^0}\left(a_6 - \frac{1}{2}a_8\right)\Big]\Big\} \\ &\quad \times A_{K^{*+}\bar{K}^0}\,, \end{aligned} \quad \text{(B.5)}$$

$$\begin{aligned} &\mathcal{A}_a^{\mathrm{SM}}(B^+\to K^{*+}\bar{K}^0) \\ &= \frac{G_\mathrm{F}}{\sqrt{2}}f_B f_K f_{K^*}\Big\{V_{ub}^*V_{ud}b_2(K^{*+},\bar{K}^0) \\ &\quad - V_{tb}^*V_{td}\Big[b_3(K^{*+},\bar{K}^0) + b_3^{\mathrm{EW}}(K^{*+},\bar{K}^0)\Big]\Big\}, \end{aligned} \quad \text{(B.6)}$$

$$\begin{aligned} &\mathcal{A}_f^{\mathrm{SM}}(B^+\to K^+\bar{K}^{*0}) \\ &= \frac{G_\mathrm{F}}{\sqrt{2}}\Big\{-V_{tb}^*V_{td}\Big[a_4 - \frac{1}{2}a_{10}\Big]\Big\}A_{K^+\bar{K}^{*0}}\,, \end{aligned} \quad \text{(B.7)}$$

$$\begin{aligned} &\mathcal{A}_a^{\mathrm{SM}}(B^+\to K^+\bar{K}^{*0}) \\ &= \frac{G_\mathrm{F}}{\sqrt{2}}f_B f_K f_{K^*}\Big\{V_{ub}^*V_{ud}b_2(K^+,\bar{K}^{*0}) \\ &\quad - V_{tb}^*V_{td}\Big[b_3(K^+,\bar{K}^{*0}) + b_3^{\mathrm{EW}}(K^+,\bar{K}^{*0})\Big]\Big\}, \end{aligned} \quad \text{(B.8)}$$

$$\begin{aligned} &\mathcal{A}_f^{\mathrm{SM}}(B^0\to K^{*0}\bar{K}^0) \\ &= \frac{G_\mathrm{F}}{\sqrt{2}}\Big\{-V_{tb}^*V_{td}\Big[a_4 - \frac{1}{2}a_{10} - r_\chi^{K^0}\left(a_6 - \frac{1}{2}a_8\right)\Big]\Big\} \\ &\quad \times A_{K^{*0}\bar{K}^0}\,, \end{aligned} \quad \text{(B.9)}$$

$$\mathcal{A}_a^{\rm SM}(B^0 \to K^{*0}\bar{K}^0) = \frac{G_{\rm F}}{\sqrt{2}} f_B f_K f_{K^*} \Big\{ -V_{tb}^* V_{td} \Big[b_3(K^{*0},\bar{K}^0) + b_4(K^{*0},\bar{K}^0) + b_4(\bar{K}^0,K^{*0}) - \frac{1}{2} b_3^{\rm EW}(K^{*0},\bar{K}^0) - \frac{1}{2} b_4^{\rm EW}(K^{*0},\bar{K}^0) - \frac{1}{2} b_4^{\rm EW}(\bar{K}^0,K^{*0}) \Big] \Big\}, \tag{B.10}$$

$$\mathcal{A}_f^{\rm SM}(B^0 \to K^0\bar{K}^{*0}) = \frac{G_{\rm F}}{\sqrt{2}} \Big\{ -V_{tb}^* V_{td} \Big[a_4 - \frac{1}{2} a_{10} \Big] \Big\} A_{K^0\bar{K}^{*0}}, \tag{B.11}$$

$$\mathcal{A}_a^{\rm SM}(B^0 \to K^0\bar{K}^{*0}) = \frac{G_{\rm F}}{\sqrt{2}} f_B f_K f_{K^*} \Big\{ -V_{tb}^* V_{td} \Big[b_3(K^0,\bar{K}^{*0}) + b_4(K^0,\bar{K}^{*0}) + b_4(\bar{K}^{*0},K^0) - \frac{1}{2} b_3^{\rm EW}(K^0,\bar{K}^{*0}) - \frac{1}{2} b_4^{\rm EW}(K^0,\bar{K}^{*0}) - \frac{1}{2} b_4^{\rm EW}(\bar{K}^{*0},K^0) \Big] \Big\}, \tag{B.12}$$

$$\mathcal{A}_f^{\rm SM}(B^+ \to K^{*+}\bar{K}^{*0}) = \frac{G_{\rm F}}{\sqrt{2}} \Big\{ -V_{tb}^* V_{td} \Big[a_4 - \frac{1}{2} a_{10} \Big] \Big\} A_{K^{*+}\bar{K}^{*0}}, \tag{B.13}$$

$$\mathcal{A}_f^{\rm SM}(B^0 \to K^{*0}\bar{K}^{*0}) = \frac{G_{\rm F}}{\sqrt{2}} \Big\{ -V_{tb}^* V_{td} \Big[a_4 - \frac{1}{2} a_{10} \Big] \Big\} A_{K^{*0}\bar{K}^{*0}}. \tag{B.14}$$

Here we have not considered the annihilation contributions in the $B \to VV$ decays.

Appendix C: The amplitudes for RPV

We have

$$\mathcal{A}^{\not R_p}(B^+ \to K^+\bar{K}^0) = \Big\{ \frac{\lambda''_{i23}\lambda''^*_{i12}}{16m^2_{\tilde{u}_i}} \eta^{-4/\beta_0} F_{K^+\bar{K}^0} + \Big(\frac{\lambda'_{i13}\lambda'^*_{i22}}{8m^2_{\tilde{\nu}_{{\rm L}i}}} - \frac{\lambda'_{i22}\lambda'^*_{i31}}{8m^2_{\tilde{\nu}_{{\rm L}i}}} \Big) \eta^{-8/\beta_0} L_{K^+\bar{K}^0} + \Big(\frac{\lambda'_{i12}\lambda'^*_{i32}}{8m^2_{\tilde{\nu}_{{\rm L}i}}} - \frac{\lambda'_{i23}\lambda'^*_{i21}}{8m^2_{\tilde{\nu}_{{\rm L}i}}} \Big) \eta^{-8/\beta_0} r_\chi^{K^0} \Big\} A_{K^+\bar{K}^0}, \tag{C.1}$$

$$\mathcal{A}^{\not R_p}(B^0 \to K^0\bar{K}^0) = \Big\{ \frac{\lambda''_{i23}\lambda''^*_{i12}}{16m^2_{\tilde{u}_i}} \eta^{-4/\beta_0} F_{K^0\bar{K}^0} + \Big(\frac{\lambda'_{i13}\lambda'^*_{i22}}{8m^2_{\tilde{\nu}_{{\rm L}i}}} - \frac{\lambda'_{i22}\lambda'^*_{i31}}{8m^2_{\tilde{\nu}_{{\rm L}i}}} \Big) \eta^{-8/\beta_0} L_{K^0\bar{K}^0} + \Big(\frac{\lambda'_{i12}\lambda'^*_{i32}}{8m^2_{\tilde{\nu}_{{\rm L}i}}} - \frac{\lambda'_{i23}\lambda'^*_{i21}}{8m^2_{\tilde{\nu}_{{\rm L}i}}} \Big) \eta^{-8/\beta_0} r_\chi^{K^0} \Big\} A_{K^0\bar{K}^0}, \tag{C.2}$$

$$\mathcal{A}^{\not R_p}(B^+ \to K^{*+}\bar{K}^0) = \Big\{ \frac{\lambda''_{i23}\lambda''^*_{i12}}{16m^2_{\tilde{u}_i}} \eta^{-4/\beta_0} F_{K^{*+}\bar{K}^0} + \Big(\frac{\lambda'_{i13}\lambda'^*_{i22}}{8m^2_{\tilde{\nu}_{{\rm L}i}}} + \frac{\lambda'_{i22}\lambda'^*_{i31}}{8m^2_{\tilde{\nu}_{{\rm L}i}}} \Big) \eta^{-8/\beta_0} (-L_{K^{*+}\bar{K}^0}) - \Big(\frac{\lambda'_{i12}\lambda'^*_{i32}}{8m^2_{\tilde{\nu}_{{\rm L}i}}} + \frac{\lambda'_{i23}\lambda'^*_{i21}}{8m^2_{\tilde{\nu}_{{\rm L}i}}} \Big) \eta^{-8/\beta_0} r_\chi^{K^0} \Big\} A_{K^{*+}\bar{K}^0}, \tag{C.3}$$

$$\mathcal{A}^{\not R_p}(B^+ \to K^+\bar{K}^{*0}) = \Big\{ \frac{\lambda''_{i23}\lambda''^*_{i12}}{16m^2_{\tilde{u}_i}} \eta^{-4/\beta_0} F_{K^+\bar{K}^{*0}} + \Big(\frac{\lambda'_{i13}\lambda'^*_{i22}}{8m^2_{\tilde{\nu}_{{\rm L}i}}} + \frac{\lambda'_{i22}\lambda'^*_{i31}}{8m^2_{\tilde{\nu}_{{\rm L}i}}} \Big) \eta^{-8/\beta_0} L_{K^+\bar{K}^{*0}} \Big\} A_{K^+\bar{K}^{*0}}, \tag{C.4}$$

$$\mathcal{A}^{\not R_p}(B^0 \to K^{*0}\bar{K}^0) = \Big\{ \frac{\lambda''_{i23}\lambda''^*_{i12}}{16m^2_{\tilde{u}_i}} \eta^{-4/\beta_0} F_{K^{*0}\bar{K}^0} + \Big(\frac{\lambda'_{i13}\lambda'^*_{i22}}{8m^2_{\tilde{\nu}_{{\rm L}i}}} + \frac{\lambda'_{i22}\lambda'^*_{i31}}{8m^2_{\tilde{\nu}_{{\rm L}i}}} \Big) \eta^{-8/\beta_0} (-L_{K^{*0}\bar{K}^0}) - \Big(\frac{\lambda'_{i12}\lambda'^*_{i32}}{8m^2_{\tilde{\nu}_{{\rm L}i}}} + \frac{\lambda'_{i23}\lambda'^*_{i21}}{8m^2_{\tilde{\nu}_{{\rm L}i}}} \Big) \eta^{-8/\beta_0} r_\chi^{K^0} \Big\} A_{K^{*0}\bar{K}^0}, \tag{C.5}$$

$$\mathcal{A}^{\not R_p}(B^0 \to K^0\bar{K}^{*0}) = \Big\{ \frac{\lambda''_{i23}\lambda''^*_{i12}}{16m^2_{\tilde{u}_i}} \eta^{-4/\beta_0} F_{K^0\bar{K}^{*0}} + \Big(\frac{\lambda'_{i13}\lambda'^*_{i22}}{8m^2_{\tilde{\nu}_{{\rm L}i}}} + \frac{\lambda'_{i22}\lambda'^*_{i31}}{8m^2_{\tilde{\nu}_{{\rm L}i}}} \Big) \eta^{-8/\beta_0} L_{K^0\bar{K}^{*0}} \Big\} A_{K^0\bar{K}^{*0}}, \tag{C.6}$$

$$\mathcal{A}^{\not R_p}(B^+ \to K^{*+}\bar{K}^{*0}) = \Big\{ \frac{\lambda''_{i23}\lambda''^*_{i12}}{16m^2_{\tilde{u}_i}} \eta^{-4/\beta_0} F'_{K^{*+}\bar{K}^{*0}} + \Big(\frac{\lambda'_{i13}\lambda'^*_{i22}}{8m^2_{\tilde{\nu}_{{\rm L}i}}} \Big) \eta^{-8/\beta_0} L'_{K^{*+}\bar{K}^{*0}} \Big\} A'_{K^{*+}\bar{K}^{*0}} + \frac{\lambda'_{i22}\lambda'^*_{i31}}{8m^2_{\tilde{\nu}_{{\rm L}i}}} L_{K^{*+}\bar{K}^{*0}} A_{K^{*+}\bar{K}^{*0}}, \tag{C.7}$$

$$\mathcal{A}^{\not R_p}(B^+ \to K^{*0}\bar{K}^{*0}) = \Big\{ \frac{\lambda''_{i23}\lambda''^*_{i12}}{16m^2_{\tilde{u}_i}} \eta^{-4/\beta_0} F'_{K^{*0}\bar{K}^{*0}} + \Big(\frac{\lambda'_{i13}\lambda'^*_{i22}}{8m^2_{\tilde{\nu}_{{\rm L}i}}} \Big) \eta^{-8/\beta_0} L'_{K^{*0}\bar{K}^{*0}} \Big\} A'_{K^{*0}\bar{K}^{*0}} + \frac{\lambda'_{i22}\lambda'^*_{i31}}{8m^2_{\tilde{\nu}_{{\rm L}i}}} L_{K^{*0}\bar{K}^{*0}} A_{K^{*0}\bar{K}^{*0}}. \tag{C.8}$$

In $\mathcal{A}^{\not R_p}$, $F^{(\prime)}_{M_1M_2}$ and $L^{(\prime)}_{M_1M_2}$ are defined as

$$F_{M_1M_2} \equiv 1 - \frac{1}{N_C} + \frac{\alpha_{\rm s}}{4\pi} \frac{C_F}{N_C} \Big[V_{M_2} + H_{M_1M_2} \Big], \tag{C.9}$$

$$L_{M_1M_2} \equiv \frac{1}{N_C}\left\{1-\frac{\alpha_s}{4\pi}\frac{C_F}{N_C}\left[12+V_{M_2}+H_{M_1M_2}\right]\right\}, \tag{C.10}$$

for $B \to PP, PV$ decays, and

$$F'_{M_1M_2} \equiv 1-\frac{1}{N_C}-\frac{\alpha_s}{4\pi}\frac{C_F}{N_C}\left[V'^{\lambda}_{M_2}(-1)+H'^{\lambda}_{M_1M_2}(-1)\right], \tag{C.11}$$

$$L'_{M_1M_2} \equiv \frac{1}{N_C}\left\{1+\frac{\alpha_s}{4\pi}\frac{C_F}{N_C}\left[-12+V'^{\lambda}_{M_2}(1)+H'^{\lambda}_{M_1M_2}(1)\right]\right\}, \tag{C.12}$$

$$L_{M_1M_2} \equiv \frac{1}{N_C}\left\{1-\frac{\alpha_s}{4\pi}\frac{C_F}{N_C}\left[12+V^{\lambda}_{M_2}(-1)+H^{\lambda}_{M_1M_2}(-1)\right]\right\}, \tag{C.13}$$

for $B \to VV$ decays.

References

1. A.J. Buras et al., Phys. Rev. Lett. **92**, 101 804 (2004); Nucl. Phys. B **697**, 133 (2004)
2. BABAR Collaboration, B. Aubert et al., Phys. Rev. Lett. **93**, 231 804 (2004); Belle Collaboration, K.F. Chen et al., Phys. Rev. Lett. **94**, 221 804 (2005)
3. S. Weinberg, Phys. Rev. D **26**, 287 (1982); N. Sakai, T. Yanagida, Nucl. Phys. B **197**, 533 (1982); C. Aulakh, R. Mohapatra, Phys. Lett. B **119**, 136 (1982)
4. See, for example, R. Barbier et al., Phys. Rept. **420**, 1 (2005) [hep-ph/9810232], and references therein; M. Chemtob, Prog. Part. Nucl. Phys. **54**, 71 (2005)
5. B.C. Allanach et al., hep-ph/9906224, and references therein.
6. G. Bhattacharyya, A. Raychaudhuri, Phys. Rev. D **57**, R3837 (1998); D. Guetta, Phys. Rev. D **58**, 116 008 (1998); G. Bhattacharyya, A. Datta, Phys. Rev. Lett. **83**, 2300 (1999); G. Bhattacharyya, A. Datta, A. Kundu, Phys. Lett. B **514**, 47 (2001); D. Chakraverty, D. Choudhury, Phys. Rev. D **63**, 075 009 (2001); D. Chakraverty, D. Choudhury, Phys. Rev. D **63**, 112 002 (2001); J.P. Saha, A. Kundu, Phys. Rev. D **66**, 054 021 (2002); D. Choudhury, B. Dutta, A. Kundu, Phys. Lett. B **456**, 185 (1999); G. Bhattacharyya, A. Datta, A. Kundu, J. Phys. G **30**, 1947 (2004); B. Dutta, C.S. Kim, S. Oh, Phys. Rev. Lett. **90**, 011 801 (2003); A. Datta, Phys. Rev. D **66**, 071 702 (2002); C. Dariescu, M.A. Dariescu, N.G. Deshpande, D.K. Ghosh, Phys. Rev. D **69**, 112 003 (2004); S. Bar-Shalom, G. Eilam, Y.D. Yang, Phys. Rev. D **67**, 014 007 (2003)
7. D.K. Ghosh, X.G. He, B.H.J. McKellar, J.Q. Shi, JHEP **0207**, 067 (2002)
8. Y.D. Yang, R.M. Wang, G.R. Lu, Phys. Rev. D **72**, 015 009 (2005); Phys. Rev. D **73**, 015 003 (2006)
9. J. Zhu, Y.L. Shen, C.D. Lü, Phys. Rev. D **72**, 054 015 (2005); C.D. Lü, Y.L. Shen, W. Wang, Phys. Rev. D **73**, 034 005 (2006); J.F. Cheng, Y.N. Gao, C.S. Huang, X.H. Wu, hep- ph/0512268; C.W. Bauer, I.Z. Rothstein, I.W. Stewart, hep-ph/0510241; A. Datta, D. London, Phys. Lett. B **533**, 65 (2002)
10. M. Beneke, G. Buchalla, M. Neubert, C.T. Sachrajda, Phys. Rev. Lett. **83**, 1914 (1999); Nucl. Phys. B **591**, 313 (2000); Nucl. Phys. B **606**, 245 (2001)
11. G. Buchalla, A.J. Buras, M.E. Lauteubacher, Rev. Mod. Phys. **68**, 1125 (1996)
12. M. Wirbel, B. Stech, M. Bauer, Zeit. Phys. C **29**, 637 (1985); M. Bauer, B. Stech, M. Wirbel, Zeit. Phys. C **34**, 103 (1987)
13. A. Ali et al., Phys. Rev. D **D58**, 094 009 (1998); Phys. Rev. D **59**, 014 005 (1999)
14. Y.Y. Keum, H.n. Li, A.I. Sanda, Phys. Lett. B **504**, 6 (2001); Phys. Rev. D **63**, 054 008 (2001); Y.Y. Keum, H.n. Li, Phys. Rev. D **63**, 074 006 (2001); C.D. Lü, K. Ukai, M.Z. Yang, Phys. Rev. D **63**, 074 009 (2001); Y.Y. Keum, A.I. Sanda, Phys. Rev. D **67**, 054 009 (2003)
15. P. Ball, R. Zwicky, Phys. Rev. D **71**, 014 015 (2005); Phys. Rev. D **71**, 014 029 (2005)
16. M. Beneke, G. Buchalla, M. Neubert, C.T. Sachrajda, Nucl. Phys. B **606**, 245 (2001)
17. M. Beneke, M. Neubert, Nucl. Phys. B **675**, 333 (2003)
18. S. Weinberg, Phys. Rev. D **26**, 287 (1982)
19. R. Barbier et al., Phys. Rept. **420**, 1 (2005)
20. G. Bhattacharyya, A. Datta, A. Kundu, J. Phys. G **30**, 1947 (2004)
21. S. Eidelman, et al. Phys. Lett. B **592**, 1 (2004) and 2005 partial update for the 2006 edition available on the PDG WWW pages (URL: http://pdg.lbl.gov/)
22. V.M. Braun, I.E. Filyanov, Z. Phys. C **48**, 239 (1990)
23. V.L. Chernyak, A.R. Zhitinissky, Phys. Rept. **112**, 173 (1984)
24. P. Ball, V.M. Braun, Nucl. Phys. B **543**, 201 (1999)
25. V.M. Braun, D.Yu. Ivanov, G.P. Korchemsky, Phys. Rev. D **69**, 034 014 (2004)
26. BABAR Collaboration, B. Aubert et al., Phys. Rev. Lett. **95**, 221 801 (2005); BABAR Collaboration, B. Aubert et al., hep-ex/0408080; Belle Collaboration, K. Abe et al., Phys. Rev. Lett. **95**, 231 802 (2005); CLEO Collaboration, A. Bornheim et al., Phys. Rev. D **68**, 052 002 (2003); CLEO Collaboration, R. Godang et al., Phys. Rev. Lett. **88**, 021 802 (2002)
27. Heavy Flavor Averaging Group, hep-ex/0603003
28. P.K Das, K.-C. Yang, Phys. Rev. D **71**, 094 002 (2005)
29. P. Ball et al., Nucl. Phys. B **529**, 323 (1998)
30. A. Kagan, Phys. Lett. B **601**, 151 (2004)